

Supporting Information

Control of Dominant Conduction Orbitals by Peripheral Substituents in Paddle-Wheel Diruthenium Alkynyl Molecular Junctions

Shiori Ogawa,^{a,b} Swarup Chattopadhyay,^c Yuya Tanaka,^{a,b*}, Tatsuhiko Ohto,^d Tomofumi Tada,^e Hirokazu Tada,^d Shintaro Fujii,^f Tomoaki Nishino,^f Munetaka Akita^{a,b*}

^aLaboratory for Chemistry and Life Science, Institute of Innovative Research, Tokyo Institute of Technology, 226-8503, Japan.

^b Department of Chemical Science and Engineering, School of Materials and Chemical Technology, Tokyo Institute of Technology, 226-8503, Japan.

^cDepartment of Chemistry, University of Kalyani, Nadia 741235, West Bengal, India.

^d Graduate School of Engineering Science, Osaka University
1-3 Machikaneyama, Toyonaka, Osaka 560-8531, Japan

^eKyushu University Platform of Inter/Transdisciplinary Energy Research, Research Facilities for Co-Evolutional Social Systems, Kyushu University
744 Motoooka, Nishi-ku, Fukuoka 819-0395, Japan

^fDepartment of Chemistry, School of Science, Tokyo Institute of Technology, 152-8551, Japan.

*E-mails: ytanaka@res.titech.ac.jp, akitatit@icloud.com

Table of Contents

I. General	S4
II. Synthesis	
Figure S1a. A ¹ H NMR spectrum of 1^H (500MHz, CD ₂ Cl ₂ , r.t.).	S6
Figure S1b. A ¹³ C{ ¹ H} NMR spectrum of 1^H (126 MHz, CD ₂ Cl ₂ , r.t.).	S7
Figure S1c. A ¹ H-H COSY NMR spectrum of 1^H (500MHz, CD ₂ Cl ₂ , r.t.).	S7
Figure S1d. A HSQC{ ¹ H} NMR spectrum of 1^H (500MHz, CD ₂ Cl ₂ , r.t.).	S8
Figure S1e. HR-ESI-TOF-MS spectra of 1^H (MeOH:CH ₂ Cl ₂ =1:1).	S8

Figure S1f. An IR spectrum of 1^H (ATR, neat).	S9
Figure S2a. A ¹ H NMR spectrum of 1^{Cl} (500MHz, CDCl ₃ , r.t.).	S10
Figure S2b. A ¹³ C{ ¹ H} NMR spectrum of 1^{Cl} (126 MHz, CDCl ₃ , r.t.).	S10
Figure S2c. A ¹ H-H COSY NMR spectrum of 1^{Cl} (500MHz, CDCl ₃ , r.t.).	S11
Figure S2d. A HSQC NMR spectrum of 1^{Cl} (500MHz, CDCl ₃ , r.t.).	S11
Figure S2e. A 1D NOESY NMR spectrum of 1^{Cl} (500MHz, CDCl ₃ , r.t.).	S12
Figure S2f. HR-ESI-TOF-MS spectra of 1^{Cl} (MeOH:CH ₂ Cl ₂ =1:1).	S12
Figure S2g. An IR spectrum of 1^{Cl} (ATR, neat).	S13
Figure S3a. HR-ESI-TOF-MS spectra of 2^{CF3} (MeOH:CH ₂ Cl ₂ =1:1).	S14
Figure S3b. An IR spectrum of 2^{CF3} (ATR, neat).	S14
Figure S4a. A ¹ H NMR spectrum of 1^{CF3} (500MHz, CDCl ₃ , r.t.).	S15
Figure S4b. A ¹³ C{ ¹ H} NMR spectrum of 1^{CF3} (126 MHz, CDCl ₃ , r.t.).	S16
Figure S4c. A ¹⁹ F NMR spectrum of 1^{CF3} (471 MHz, CDCl ₃ , r.t.)	S16
Figure S4d. A ¹ H-H COSY NMR spectrum of 1^{CF3} (500MHz, CDCl ₃ , r.t.).	S17
Figure S4e. A HSQC NMR spectrum of 1^{CF3} (500MHz, CDCl ₃ , r.t.).	S17
Figure S4f. A 1D NOESY NMR spectrum of 1^{CF3} (500MHz, CDCl ₃ , r.t.).	S18
Figure S4g. A 1D NOESY NMR spectrum of 1^{CF3} (500MHz, CDCl ₃ , r.t.).	S18
Figure S4h. HR-ESI-TOF-MS spectra of 1^{CF3} (MeOH).	S19
Figure S4i. An IR spectrum of 1^{CF3} (ATR, neat).	S19
Figure S5a. A ¹ H NMR spectrum of 1^{OMe} (400MHz, CD ₂ Cl ₂ , r.t.).	S20
Figure S5b. A ¹³ C{ ¹ H} NMR spectrum of 1^{OMe} (100 MHz, CD ₂ Cl ₂ , r.t.).	S21
Figure S5c. A ¹ H-H COSY NMR spectrum of 1^{OMe} (400MHz, CDCl ₃ , r.t.).	S21
Figure S5d. A HSQC NMR spectrum of 1^{OMe} (400MHz, CDCl ₃ , r.t.).	S22
Figure S5e. HR-ESI-TOF-MS spectra of 1^{OMe} (MeOH:CH ₂ Cl ₂ =1:1).	S23
Figure S5f. An IR spectrum of 1^{OMe} (ATR, neat).	S23
III. STM-BJ study	S24
Figure S6. Typical individual traces for blank experiments and 1^R (R =OMe, H, Cl, and CF ₃).	S24
Figure S7. 1D and 2D log histograms of a tetraglyme solution (a blank experiment) constructed from 2000 traces without any data selection.	S24
IV. X-ray Structures	S25

Table S1. Crystal data and structure refinement for 1^R (R=H, Cl, CF ₃).	S25
V. Vis-NIR electronic spectral study	S26
Figure S8. Vis-NIR spectra of 1^R (R = OMe, H, Cl, and CF ₃) recorded in CH ₂ Cl ₂ (1 mM). Inset shows an expanded view of the NIR region.	S26
VI. DFT study	S27
Figure S9. A part of Kohn-Sham orbitals of 1^H – 1^{CF₃} .	S27
Figure S10. Hole–particle pairs of natural transition orbitals (NTOs) of 1^H related to the visible transition bands derived from the TD-DFT calculation.	S27
Figure S11. Hole–particle pairs of natural transition orbitals (NTOs) of 1^H related to the visible transition bands derived from the TD-DFT calculation.	S28
Table S2. TD-DFT data of 1^{OMe} .	S28
Table S3. TD-DFT data of 1^H .	S29
Table S4. TD-DFT data of 1^{Cl} .	S29
Table S5. TD-DFT data of 1^{CF₃} .	S30
VII. DFT-NEGF study	S31
Figure S12. Model definition in a level-broadening approach.	S32
Figure S13. Plots of (a) experimentally (G _{exp}) and theoretically obtained conductance (G _{calc}) and (b) HOMO ^{NEGF} and LUMO ^{NEGF} against Hammett substituent constants σ. (c) Transmission spectra of of Au₁₀-1^R-Au₁₀ (R = OMe, H, Cl, and CF ₃).	S33
Table S6. Cartesian coordinates of 1^{OMe} (<i>E</i> = -4124.45439704 hartree).	S34
Table S7. Cartesian coordinates of 1^H (<i>E</i> = -4124.45439704 hartree).	S35
Table S8. Cartesian coordinates of 1^{Cl} (<i>E</i> = -7801.19753803 hartree).	S37
Table S9. Cartesian coordinates of 1^{CF₃} (<i>E</i> = -6820.73974559 hartree).	S39
VII. References	S39

I. General

Materials

Reactions were performed under N₂ atmosphere using standard Schlenk tube technique unless stated otherwise. THF and CH₂Cl₂ were purified by the Grubbs solvent purification system.^[1] 4-Ethynylthioanisole,^[2] *N,N*-bis(4-trifluoromethylphenyl)formamidine,^[3] Ru₂(OAc)₄Cl,^[4] **2^H**, and **2^{Cl}**^[5] were synthesized according to the literature procedures. Other reagents, Silica (Kanto chemical Co Inc. Silica Gel 60N), alumina (Merck Aluminum oxide 90 standardized), and Sephadex LH-20 (GE healthcare) were used as received.

Instruments

NMR spectra were recorded on a Bruker biospin ASCEND-500 spectrometer (¹H 500 MHz, ¹³C{¹H} NMR 126 MHz, ¹⁹F 471 MHz). NMR chemical shifts were referenced to the residual non-deuterated solvent signals (¹H: CHCl₃ δ = 7.26 ppm, C₆D₅H δ = 7.16 ppm, CDHCl₂ δ = 5.32 ppm, ¹³C{¹H}; CDCl₃ δ = 77 ppm), and CF₃COOH (an external reference for ¹⁹F, δ = -77.6 ppm). HR-ESI-TOF-MS measurements were performed on Bruker micrOTOF II. UV–Vis and IR spectra (KBr pellets and ATR) were obtained on JASCO V670DS and IRspirit spectrometers. Electrochemical measurements (CV and DPV) were made with Hokuto DenkoHZ-5000 (observed in CH₂Cl₂; [complex] = *ca.* 1 × 10⁻³ M; [NBu₄PF₆] = 0.1 M; working electrode: Pt, counter electrode: Pt, reference electrode: Ag/AgNO₃; scan rate: 100 mV/s (CV)). After a measurement, ferrocene (Fc) was added to the mixture, and the potentials were calibrated with respect to the Fc/Fc⁺ redox couple.

Single-Crystal X-ray Crystallography

X-ray Diffraction data was collected at 93 K under a cold nitrogen gas stream on a Rigaku XtaLaB Synergy-DW X-ray diffractometer system, using graphite-monochromated CuKα radiation (λ = 1.54184 Å). Intensity data were collected by an ω-scan with 0.5° oscillations for each frame. Bragg spots were integrated using the CrysAlis^{Pro} program package.^[6] Using Olex2,^[7] structures were solved by SHELXT^[8] and refined by SHELXL.^[9] All non-hydrogen atoms were refined with anisotropic displacement parameters. Hydrogen atoms were placed at calculated positions and refined by applying riding models. CCDC numbers 2057135-2057137 contain the supplementary crystallographic data for **1^H**, **1^{Cl}**, and **1^{CF3}**.

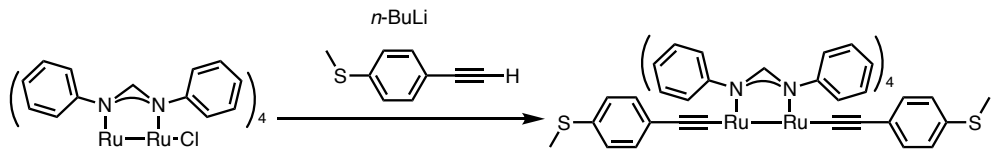
STM-BJ study

The conductance measurements were performed using electrochemical STM (Pico-SPM, Molecular Imaging Co.) and PicoScan 3000 PicoSPM II CONTROLLER (Molecular Imaging Co.). Cells, beakers, ceramic tweezers, and Schlenk tubes used for STM-BJ measurements were cleaned by soaking with mixed acid (an equivolume mixture of sulfuric acid and nitric acid) prior to use. The STM-tips were made from a gold wire (0.30 mm diameter, ca. 1.3 cm long, and 99,99% purity, obtained from The Nilaco Corporation) coated with wax (Apiezon Wax W obtained from The Nilaco Corporation). The substrate of Au(111) was formed on the surface of gold beads, which were prepared as follows. Au wires (0.90 mm diameter, ca. 5.0 cm long, and 99.99% purity, obtained from The Nilaco Corporation) were boiled in a concentrated HCl solution for more than 10 min and then rinsed with ultrapure water. Then the Au wires were flame annealed until melted into a sphere to form Au beads. The Au beads were then gently remelted until they showed single-crystalline Au(111) surface. Solutions of molecular wires in tetraglyme (0.25 mM) were used for the measurements. Conductance was measured during the breaking process under an applied bias of 100 mV. The histograms were constructed from 2000 successive traces.

DFT study

DFT and TD-DFT calculations were performed by using the Gaussian 16 program package.^[10] The complexes **1^R** (R = H, Cl, and CF₃) are optimized with the B3LYP/LanL2DZ (for Ru) and 6-31G(d) (for C, H, N, S, Cl, F) levels of theory combined with the CPCM continuum solvent method (CH₂Cl₂). Single point calculation and TD-DFT study were performed at the same level of theory.

II. Synthesis



Synthesis of **1^H.** To a solution of 4-ethynylthioanisole (666 mg, 4.50 mmol, 110 equiv.) in THF (20 mL) was added dropwise *n*-BuLi (2.45 mL of a 1.6 M solution in *n*-hexane, 3.93 mmol, 100 equiv.) at -78 °C under nitrogen atmosphere, and the mixture was stirred at room temperature for 2 h. To the reaction mixture was added a THF solution of **2^H** (41.1 mg, 0.0403 mmol, 1 equiv.; 15 mL), and the mixture was stirred overnight. Then the reaction mixture was exposed to air and stirred for 2 h. The volatiles were evaporated under reduced pressure, and the obtained residue was subjected to short silica gel column chromatography (eluted with hexane→hexane:CH₂Cl₂=9:1→CH₂Cl₂). The purple fraction eluted with CH₂Cl₂ was collected and evaporated. Then, the residue was subjected to Sephadex-LH-20 column chromatography (CH₂Cl₂). The solvent was removed in *vacuo* to afford the product as a dark purple solid (25.0 mg, 0.0196 mmol, 49 % yield).

¹H NMR: δ = 2.45 (s, 6H, SMe), 6.20 (d, *J* = 8.5 Hz, 4H, C₆H₄SMe), 6.89 (d, *J* = 7.0 Hz, 16H, C₆H₅), 6.99 (d, *J* = 8.5 Hz, 4H, C₆H₄SMe), 7.08-7.12 (m, 24H, C₆H₅), 8.27 (s, 4H, amidinate-H). ¹³C{¹H} NMR: δ = 169.2 (s, amidinate-C), 156.0 (s, C_q), 137.0 (s, C_q), 134.1 (s, C_q), 132.0 (s, C₆H₄SMe), 128.1 (s, C₆H₅), 126.1 (s, C₆H₅), 125.9 (s, C₆H₄SMe), 125.6 (s, C₆H₅), 124.9 (s, C_q), 48.67 (s, C_q), 16.47 (s, SMe). HR-ESI-TOF-MS (MeOH:CH₂Cl₂=1:1) (*m/z*): Calcd. for C₇₀H₅₈N₈Ru₂S₂: 1277.2269. Found 1277.2258 [M-H]⁻. IR (ATR, neat / cm⁻¹): 1523 (s), 1591 (s), 1952 (s), 2099 (s) *v*(C≡C), 2919 (m), 3059 (m).

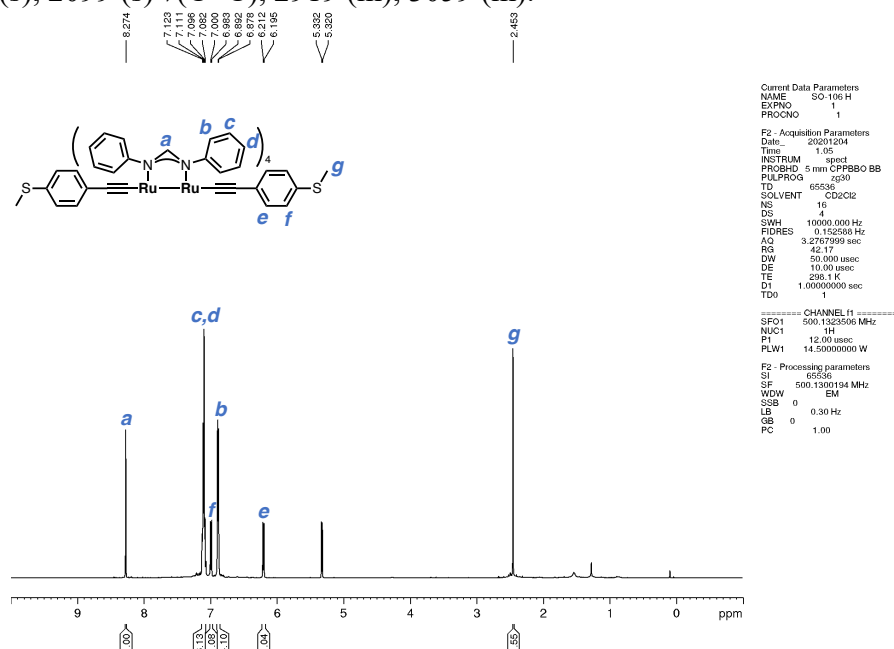


Figure S1a. A ¹H NMR spectrum of **1^H** (500MHz, CD₂Cl₂, r.t.).

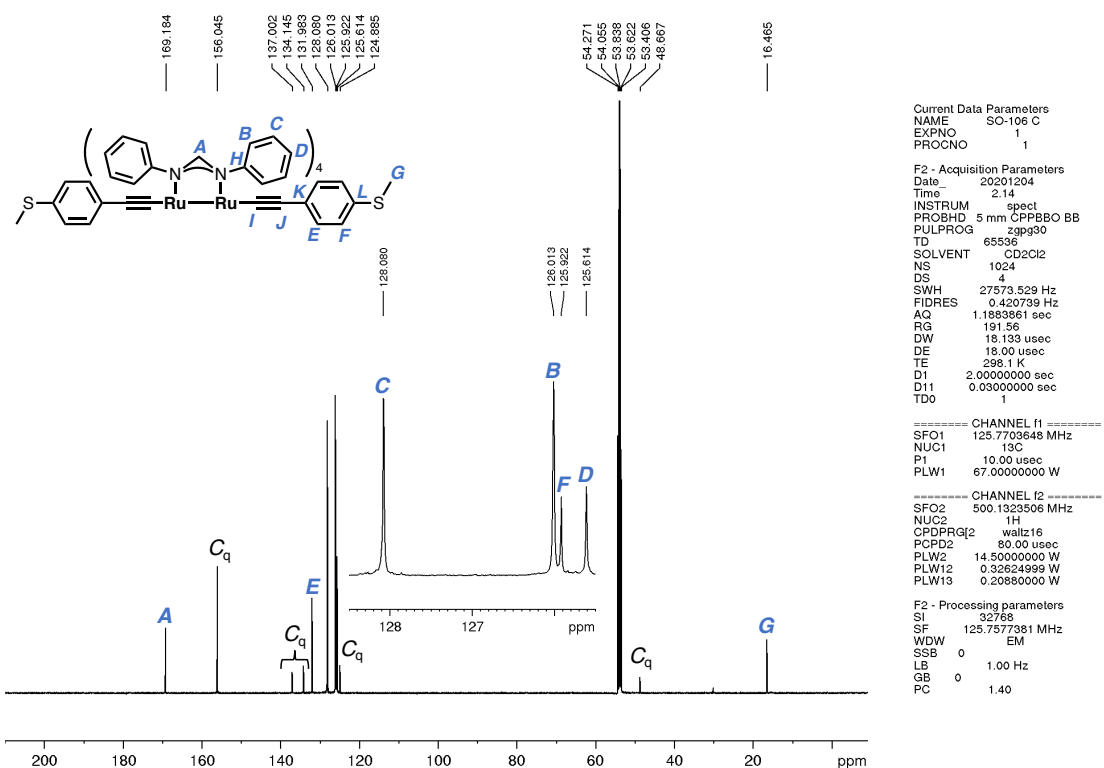


Figure S1b. A $^{13}\text{C}\{\text{H}\}$ NMR spectrum of $\mathbf{1}^{\text{H}}$ (126 MHz, CD_2Cl_2 , r.t.).

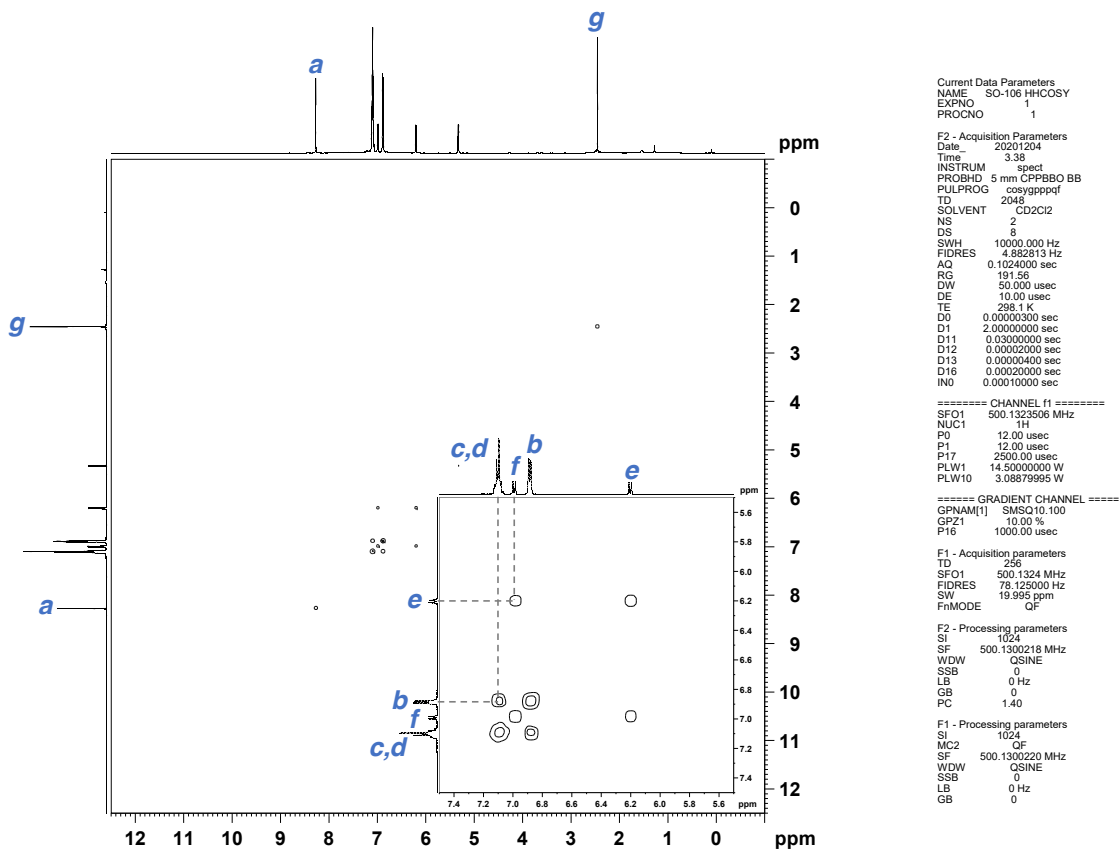


Figure S1c. A ^1H - ^1H COSY NMR spectrum of $\mathbf{1}^{\text{H}}$ (500MHz, CD_2Cl_2 , r.t.).

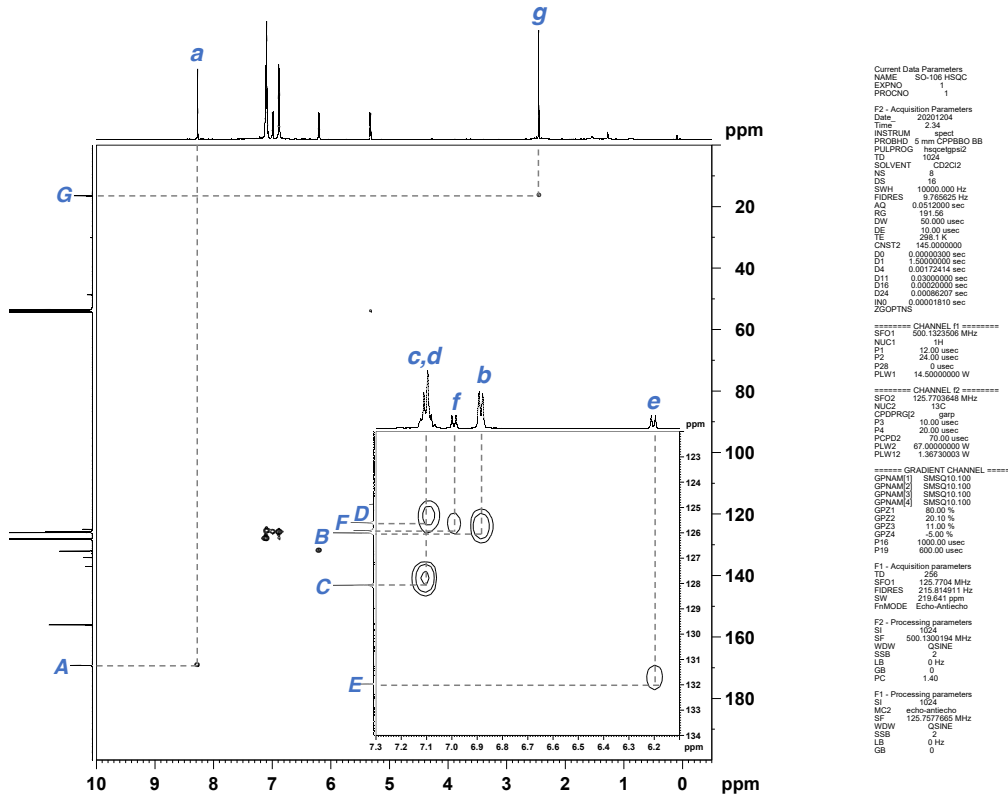


Figure S1d. A HSQC NMR spectrum of $\mathbf{1}^{\text{H}}$ (500MHz, CD_2Cl_2 , r.t.).

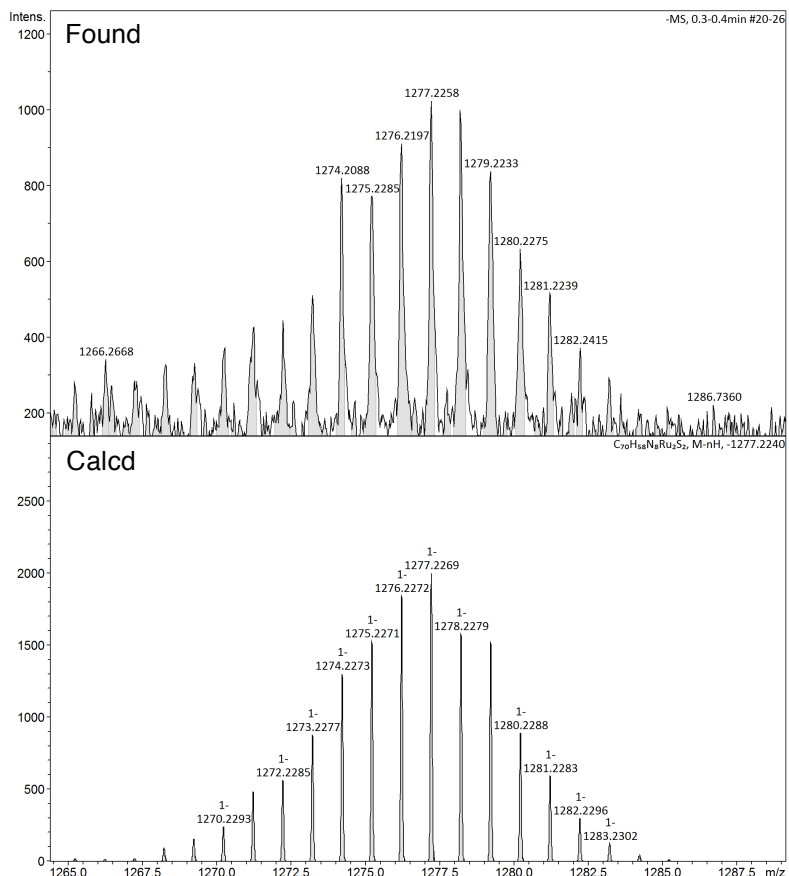


Figure S1e. HR-ESI-TOF-MS spectra of $\mathbf{1}^{\text{H}}$ ($\text{MeOH}:\text{CH}_2\text{Cl}_2 = 1:1$).

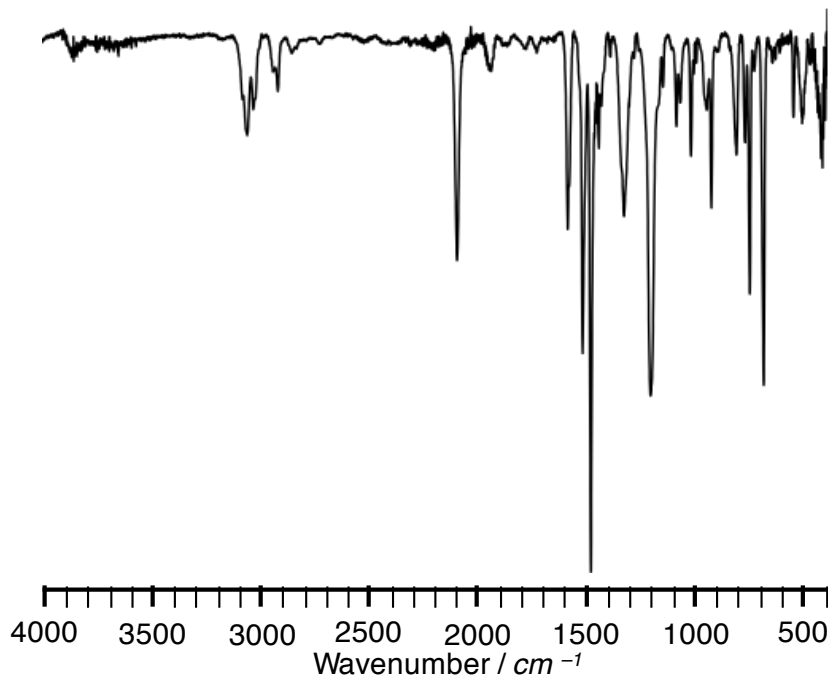
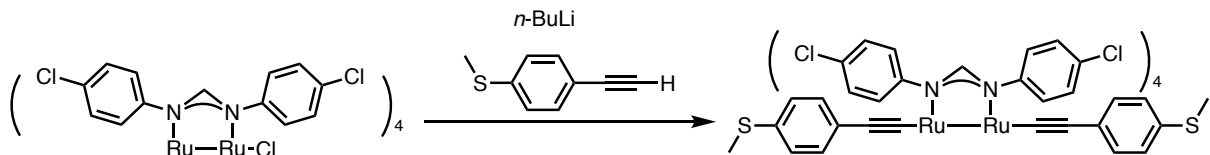


Figure S1f. An IR spectrum of $\mathbf{1}^{\mathbf{H}}$ (ATR, neat).



Synthesis of $\mathbf{1}^{\mathbf{Cl}}$. The title complex was synthesized in a manner similar to that of $\mathbf{1}^{\mathbf{H}}$ using 4-ethynylthioanisole (126 mg, 0.850 mmol, 22 equiv.), $n\text{-BuLi}$ (0.483 mL of a 1.6 M solution in $n\text{-hexane}$, 0.773 mmol, 20 equiv.), and $\mathbf{2}^{\mathbf{Cl}}$ (50.4 mg, 0.0389 mmol, 1 equiv.), and was obtained as a dark purple solid in 22 % yield (13.0 mg, 0.00837 mmol).

^1H NMR: $\delta = 2.50$ (s, 6H, SMe), 6.14 (d, $J = 8.2$ Hz, 4H, C₆H₄SMe), 6.74 (d, $J = 8.5$ Hz, 16H, C₆H₄Cl), 7.08-7.12 (m, 20H, C₆H₄Cl, C₆H₄SMe), 8.18 (s, 4H, amidinate-H). $^{13}\text{C}\{^1\text{H}\}$ NMR: $\delta = 168.5$ (s, amidinate-C), 153.4 (s, C_q), 138.9 (s, C_q), 135.2 (s, C_q), 131.6 (s, C_q), 131.4 (s, C₆H₄SMe), 128.1 (s, C₆H₄Cl), 126.3 (s, C₆H₄Cl), 125.9 (s, C₆H₄SMe), 123.3 (s, C_q), 43.45 (s, C_q), 16.14 (s, SMe). HR-ESI-TOF-MS (MeOH:CH₂Cl₂=1:1) (m/z): Calcd. for C₇₀H₅₀Cl₈N₈Ru₂S₂: 1552.9096, Found 1552.9095 [M-H]⁻. IR (ATR, neat / cm^{-1}): 1522 (s), 1587 (s), 2094 (s) $\nu(\text{C}\equiv\text{C})$, 2917 (m), 3069 (m).

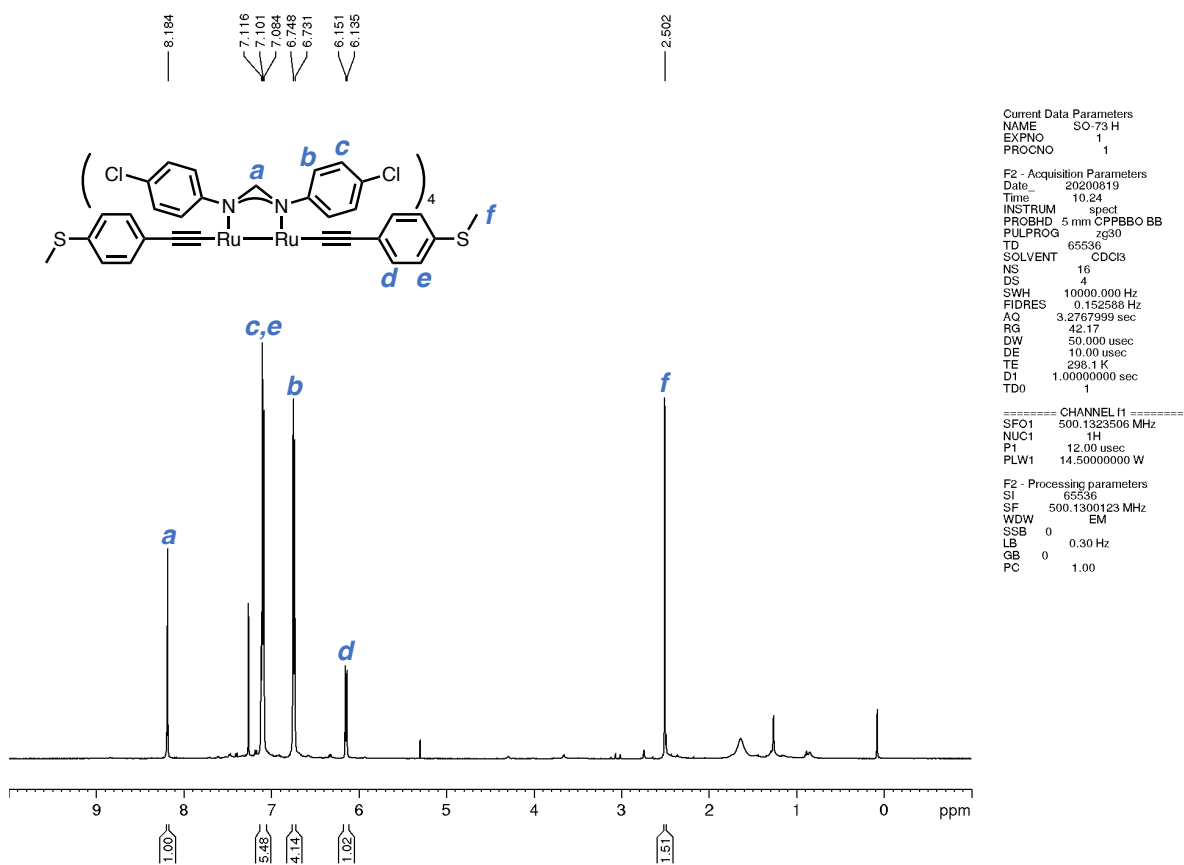


Figure S2a. A ^1H NMR spectrum of $\mathbf{1}^{\text{Cl}}$ (500MHz, CDCl_3 , r.t.).

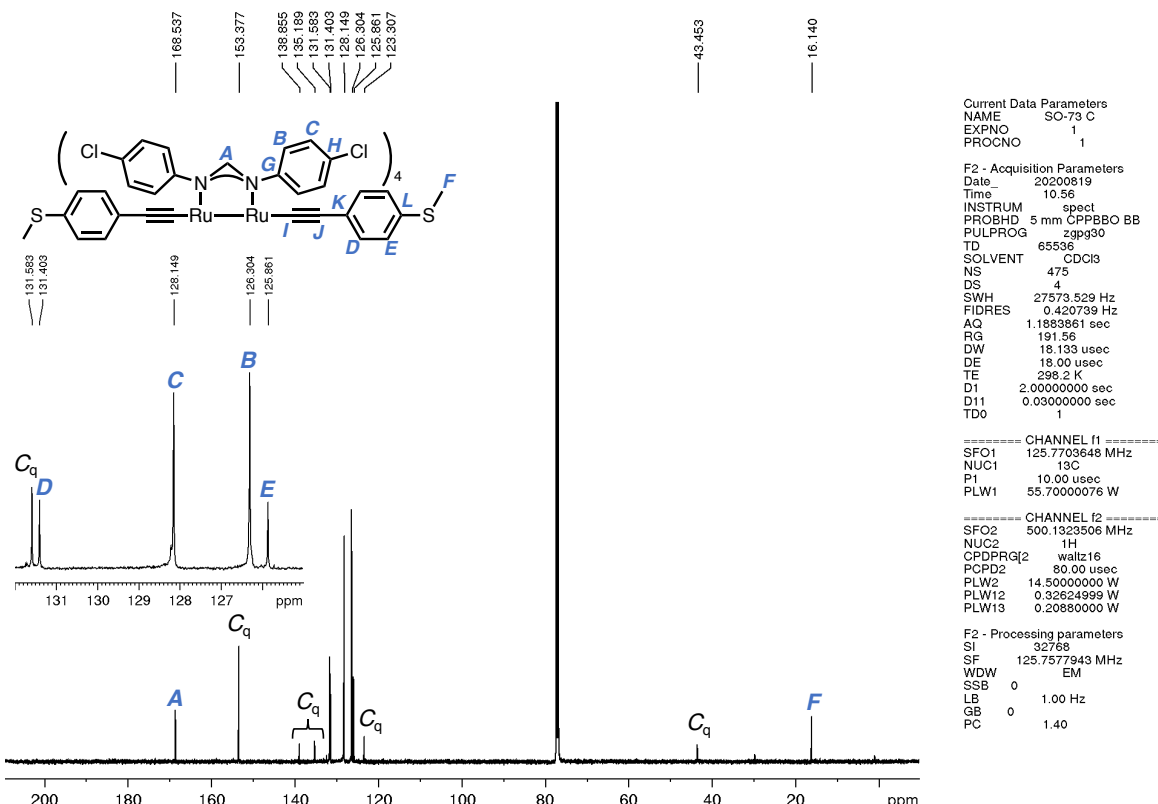


Figure S2b. A $^{13}\text{C}\{^1\text{H}\}$ NMR spectrum of $\mathbf{1}^{\text{Cl}}$ (126 MHz, CDCl_3 , r.t.).

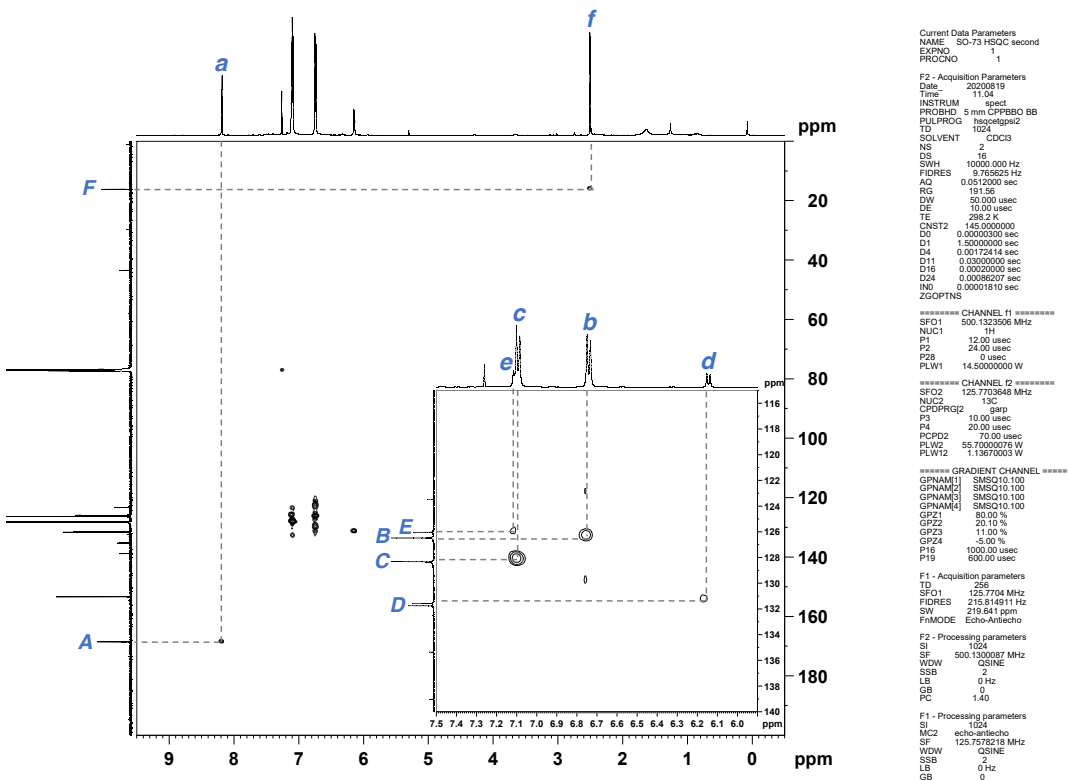


Figure S2c. A ¹H-H COSY NMR spectrum of **1^{Cl}** (500MHz, CDCl₃, r.t.).

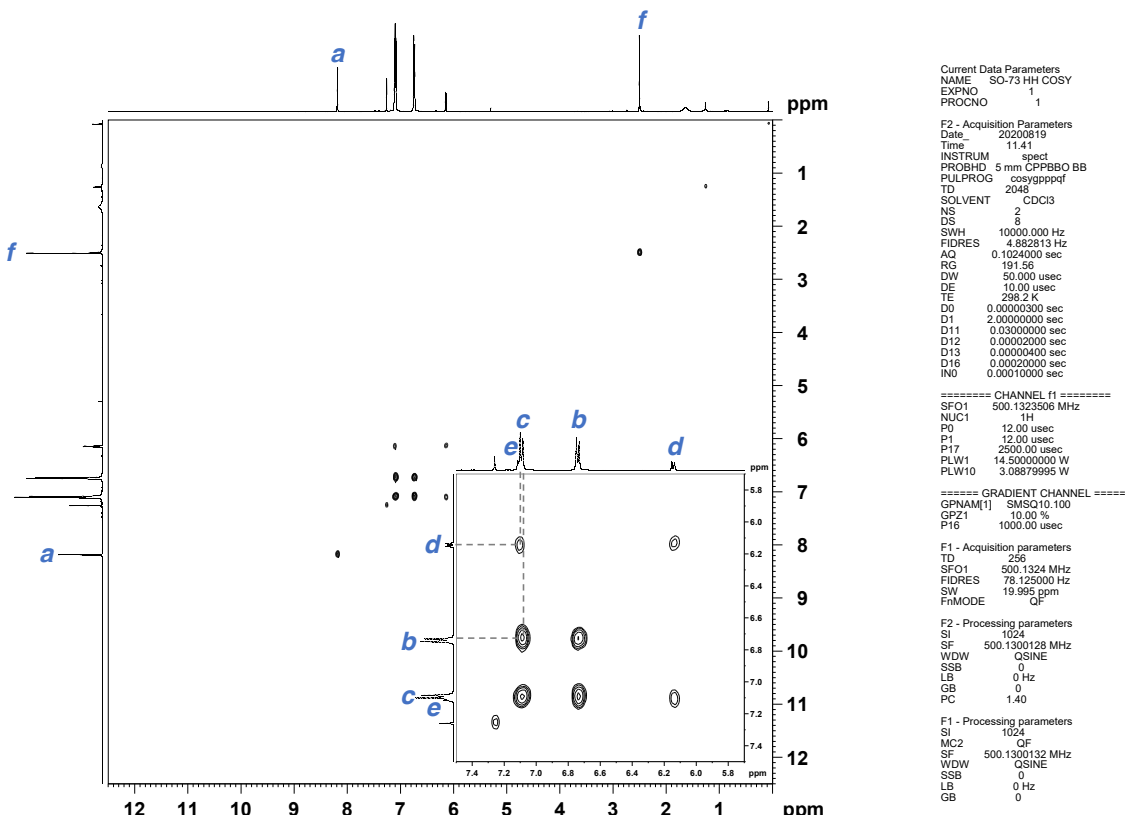


Figure S2d. A HSQC NMR spectrum of **1^{Cl}** (500MHz, CDCl₃, r.t.).

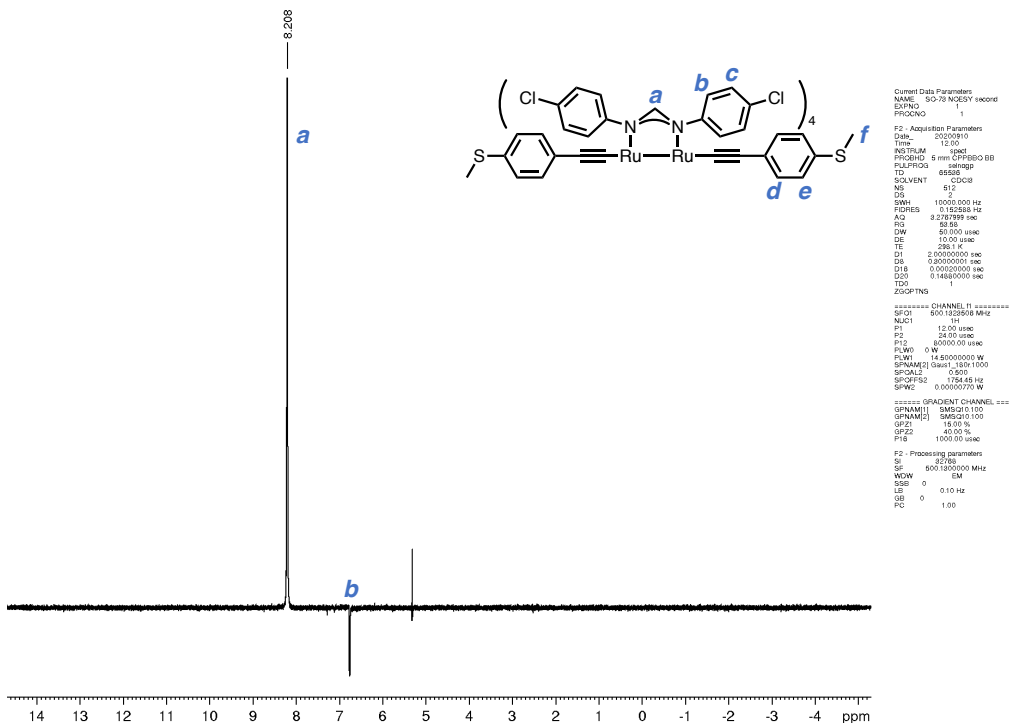


Figure S2e. A 1D NOESY NMR spectrum of **1^{Cl}** (500MHz, CDCl₃, r.t.).

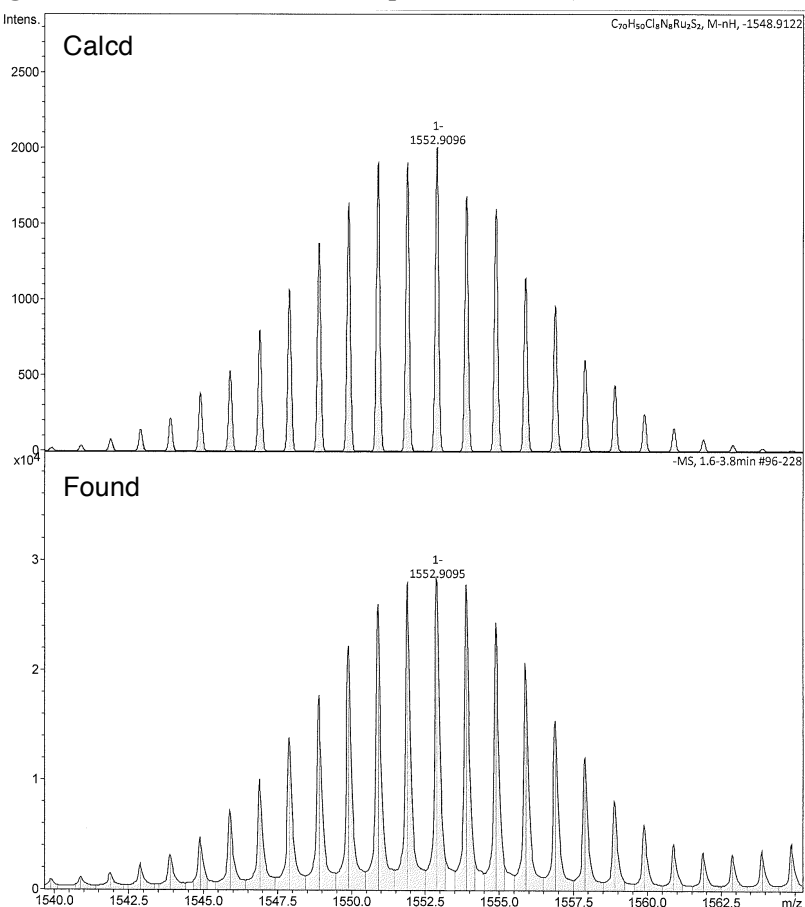


Figure S2f. HR-ESI-TOF-MS spectra of **1^{Cl}** (MeOH:CH₂Cl₂=1:1).

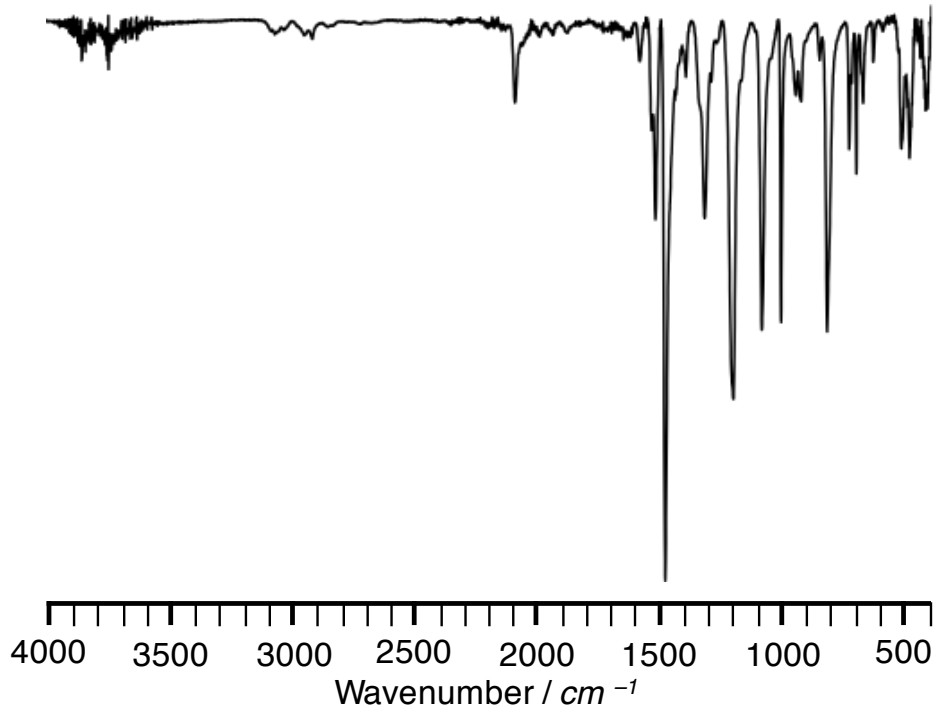
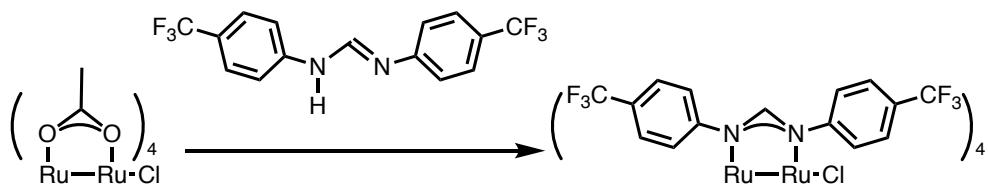


Figure S2g. An IR spectrum of $\mathbf{1}^{\text{Cl}}$ (ATR, neat).



Synthesis of $\mathbf{2}^{\text{CF}_3}$. To a mixture of $\text{N},\text{N}'\text{-bis}[4\text{-trifluoromethylphenyl}]$ methanimidamide (281 mg, 0.846 mmol, 8 equiv.) and $\text{Ru}_2(\text{OAc})_4\text{Cl}$ (49.6 mg, 0.105 mmol, 1 equiv.) was heated at 175°C for 4 h under nitrogen atmosphere. The reaction mixture was allowed to cool to room temperature, and ethanol (10 mL) was added to the mixture. The resulting suspension was filtered, and the residue was dried in *vacuo* to afford greenish black crystals (91.0 mg, 0.0582 mmol, 55% yield). HR-ESI-TOF-MS (MeOH:CH₂Cl₂=1:1) (*m/z*): Calcd. for. C₆₀H₃₆ClF₂₄N₈Ru₂: 1563.0483, Found 1563.0475 [M]⁻. IR (ATR, neat / cm⁻¹): 1016 (s), 1066 (s), 1107 (m), 1165 (s), 1224 (s), 1319 (s), 1411 (s), 1509 (s), 1539 (s), 1612 (s).

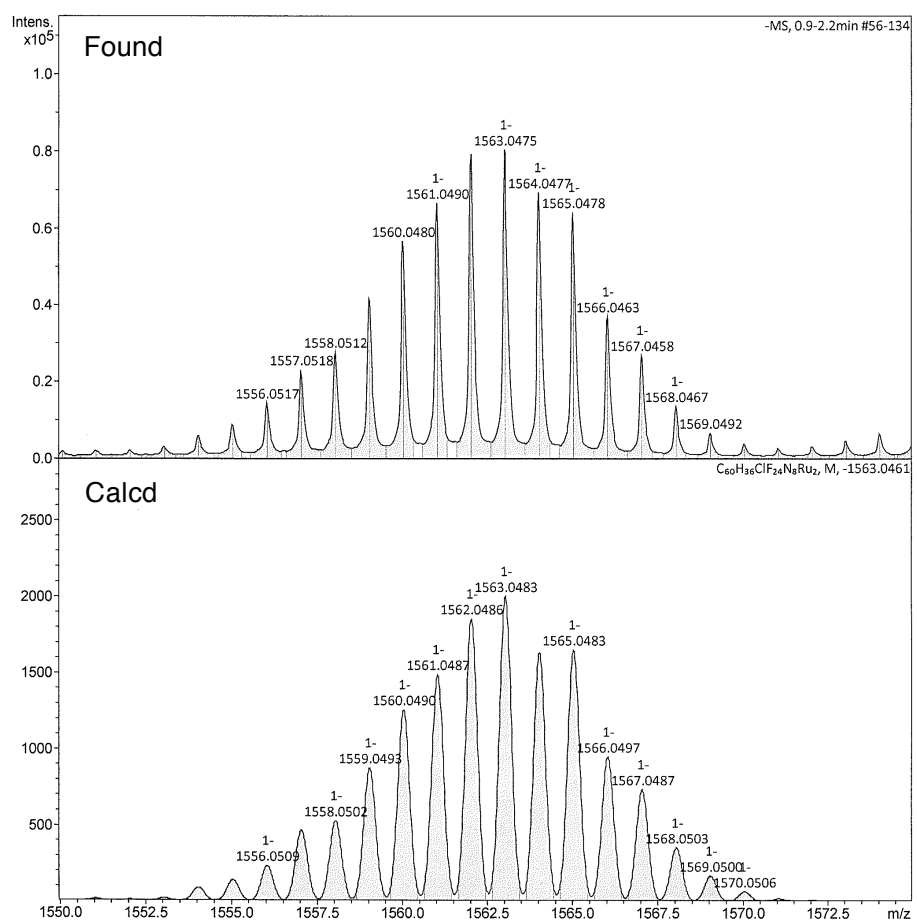


Figure S3a. HR-ESI-TOF-MS spectra of $\mathbf{2}^{\text{CF}_3}$ (MeOH:CH₂Cl₂=1:1).

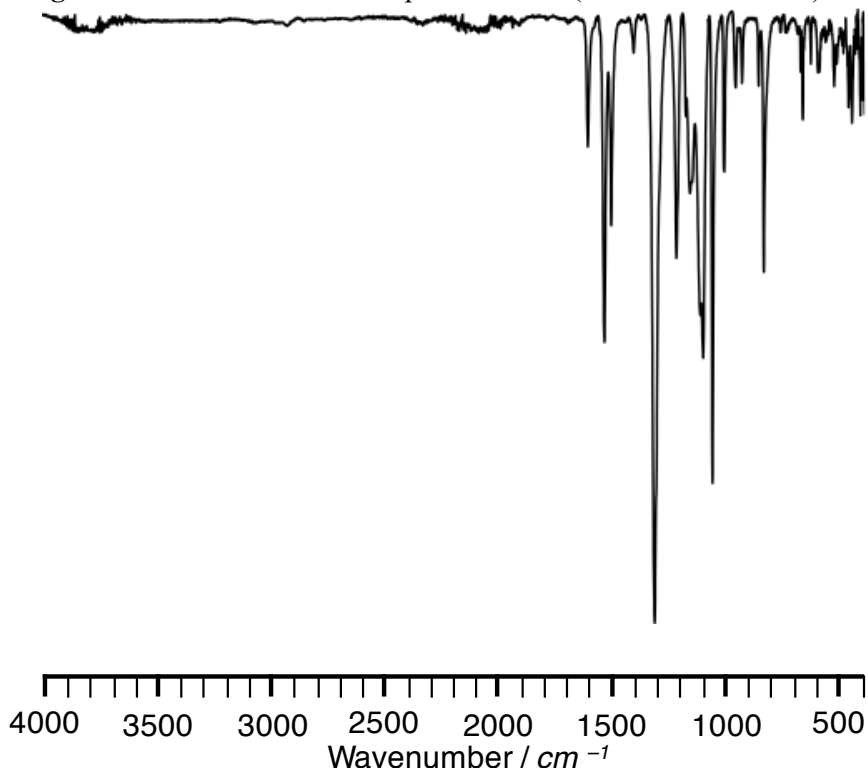
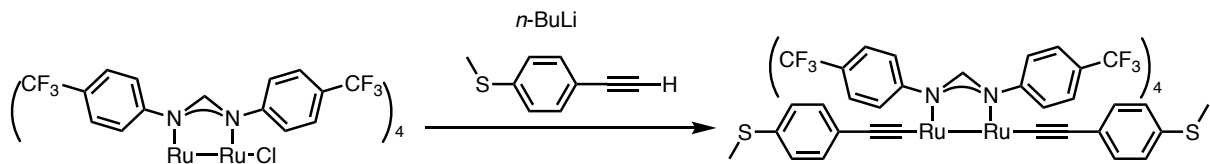


Figure S3b. An IR spectrum of $\mathbf{2}^{\text{CF}_3}$ (ATR, neat).



Synthesis of $\mathbf{1}^{\text{CF}_3}$. The title complex was synthesized in a manner similar to that of $\mathbf{1}^{\text{H}}$ using 4-ethynylthioanisole (303 mg, 2.05 mmol, 22 equiv.), $n\text{-BuLi}$ (1.12 mL of a 1.6 M solution in n -hexane, 1.80 mmol, 20 equiv.), and $\mathbf{2}^{\text{CF}_3}$ (141 mg, 0.0899 mmol, 1 equiv.), and was obtained as a dark purple solid in 17 % yield (27.7 mg, 0.0152 mmol).

^1H NMR: $\delta = 2.47$ (s, 6H, SMe), 5.93 (d, $J = 8.5$ Hz, 4H, $\text{C}_6\text{H}_4\text{SMe}$), 6.98 (d, $J = 8.0$ Hz, 16H, $\text{C}_6\text{H}_4\text{CF}_3$), 7.01 (d, $J = 8.5$ Hz, 4H, $\text{C}_6\text{H}_4\text{SMe}$), 7.41 (d, $J = 8.0$ Hz, 16H, $\text{C}_6\text{H}_4\text{CF}_3$), 8.37 (s, 4H, amidinate-H). $^{13}\text{C}\{\text{H}\}$ NMR: $\delta = 169.2$ (s, amidinate-C), 157.2 (s, C_q), 140.7 (s, C_q), 136.7 (s, C_q), 131.4 (s, $\text{C}_6\text{H}_4\text{SMe}$), 128.4 (q, $J = 32.90$ Hz, $\text{C}_6\text{H}_4\text{CF}_3$), 123.8 (q, $J = 272.8$ Hz, CF_3), 125.6 (s, $\text{C}_6\text{H}_4\text{SMe}$), 125.6 (s, $\text{C}_6\text{H}_4\text{CF}_3$), 125.3 (s, $\text{C}_6\text{H}_4\text{CF}_3$), 122.2 (s, C_q), 40.85 (s, C_q), 15.97 (s, SMe). ^{19}F NMR: $\delta = -62.8$ (s, CF_3). HR-ESI-TOF-MS (MeOH) (m/z): Calcd. for. $\text{C}_{78}\text{H}_{50}\text{F}_{24}\text{N}_8\text{Ru}_2\text{S}_2$: 1821.1263, Found 1821.1230 [M-H] $^-$. IR (ATR, neat / cm^{-1}): 1507 (m), 1611 (s), 2101 (m) $\nu(\text{C}\equiv\text{C})$.

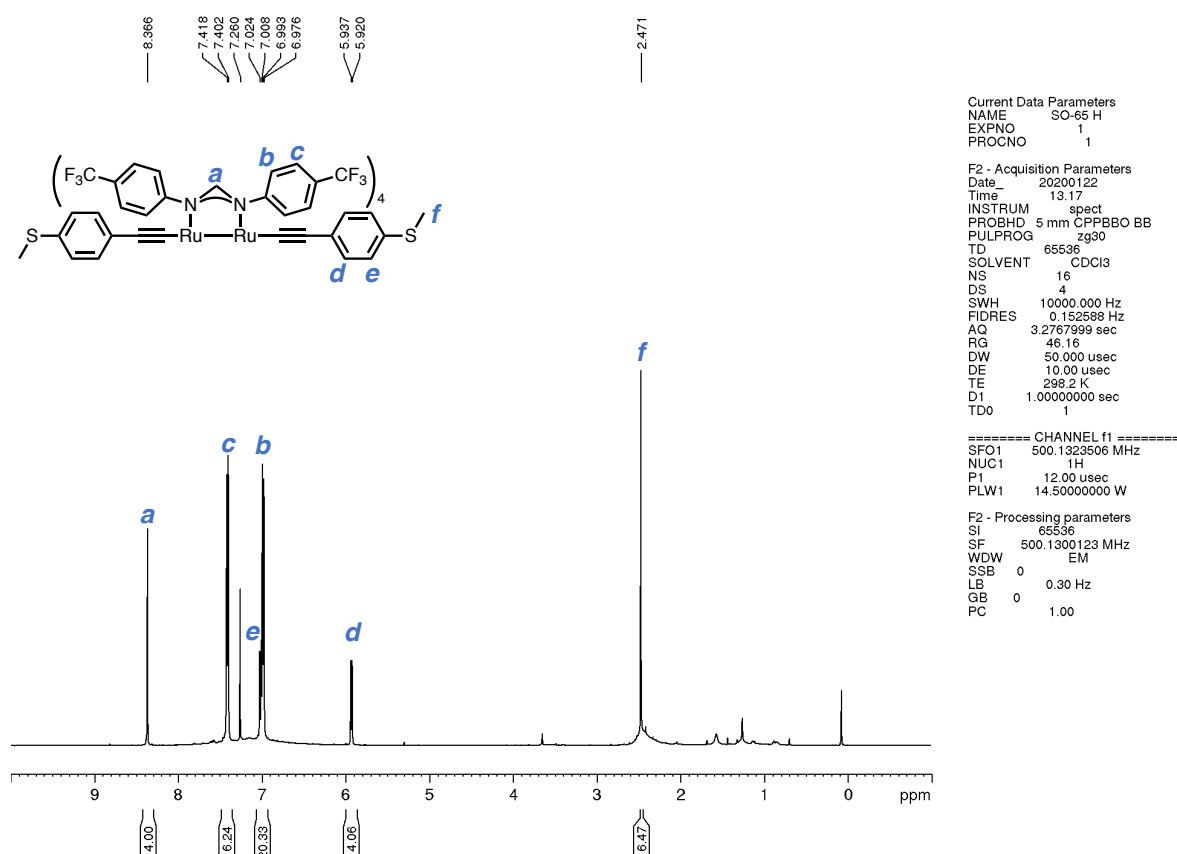


Figure S4a. A ^1H NMR spectrum of $\mathbf{1}^{\text{CF}_3}$ (500MHz, CDCl₃, r.t.).

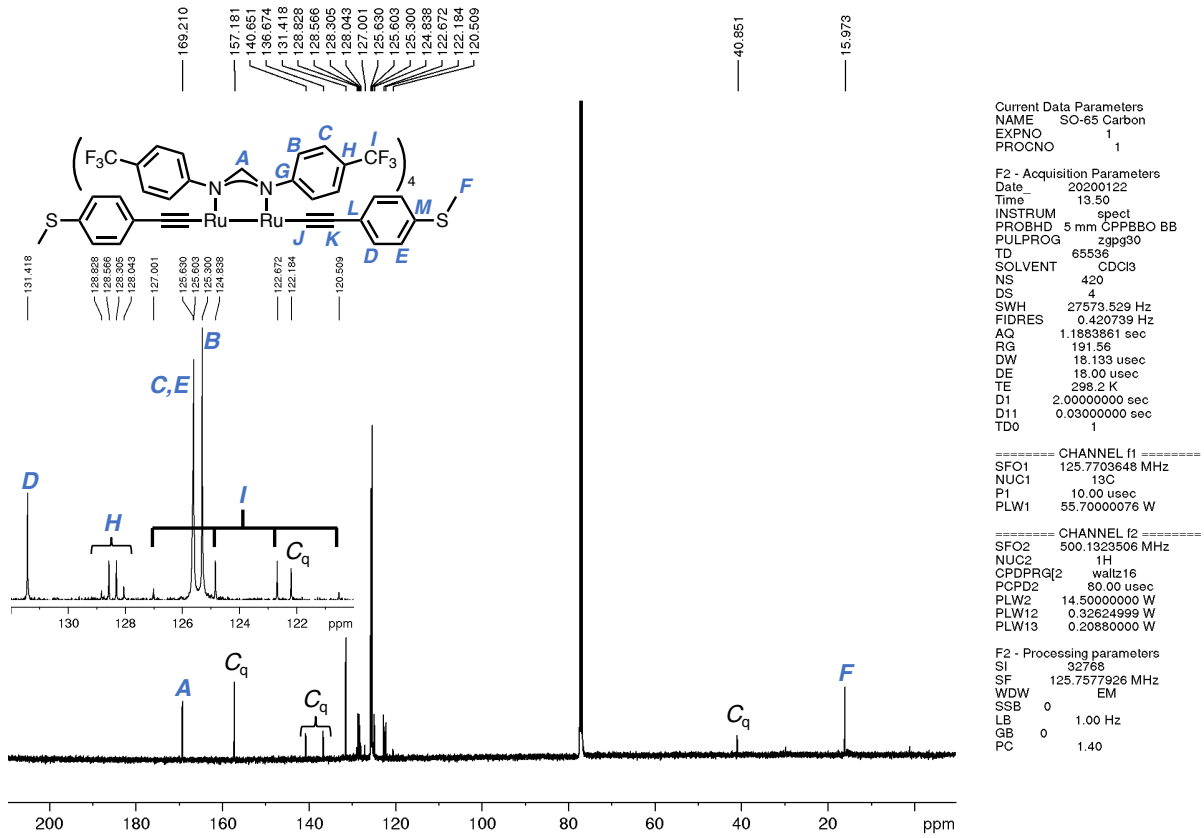


Figure S4b. A $^{13}\text{C}\{\text{H}\}$ NMR spectrum of $\mathbf{1}^{\text{CF}_3}$ (126 MHz, CDCl₃, r.t.).

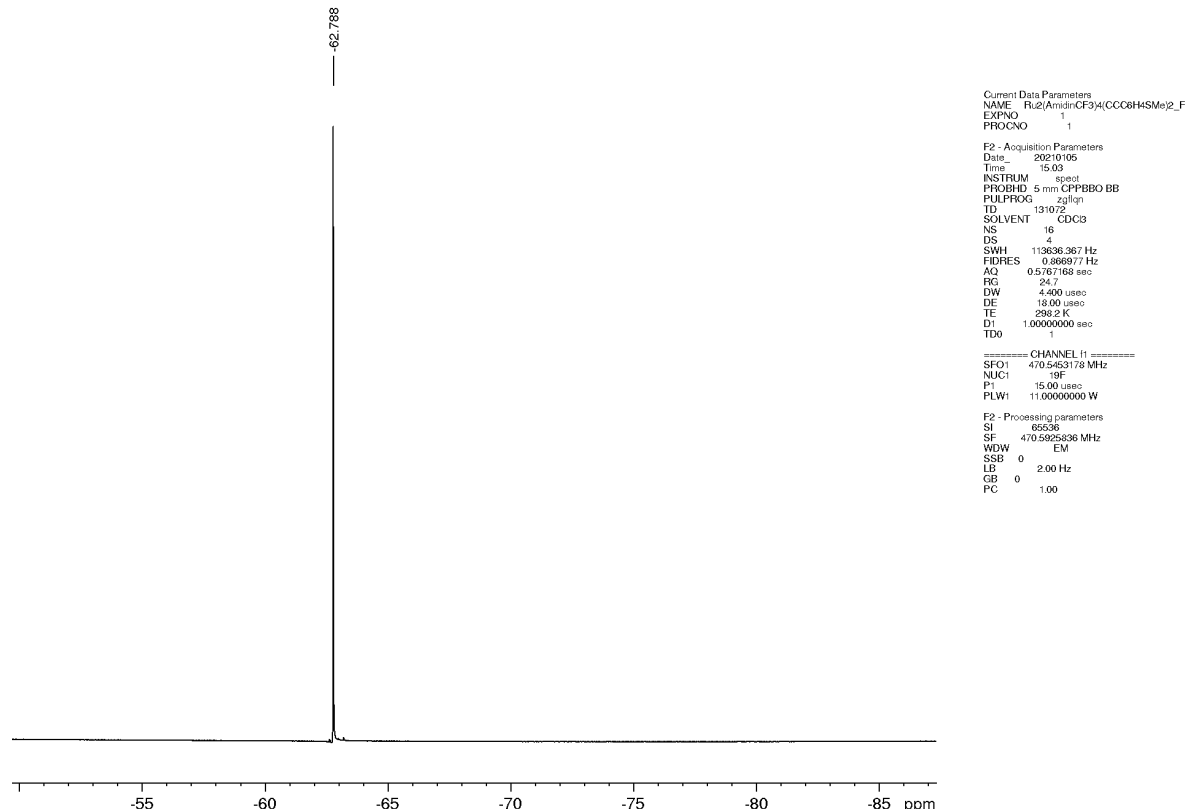


Figure S4c. A ^{19}F NMR spectrum of $\mathbf{1}^{\text{CF}_3}$ (471 MHz, CDCl₃, r.t.)

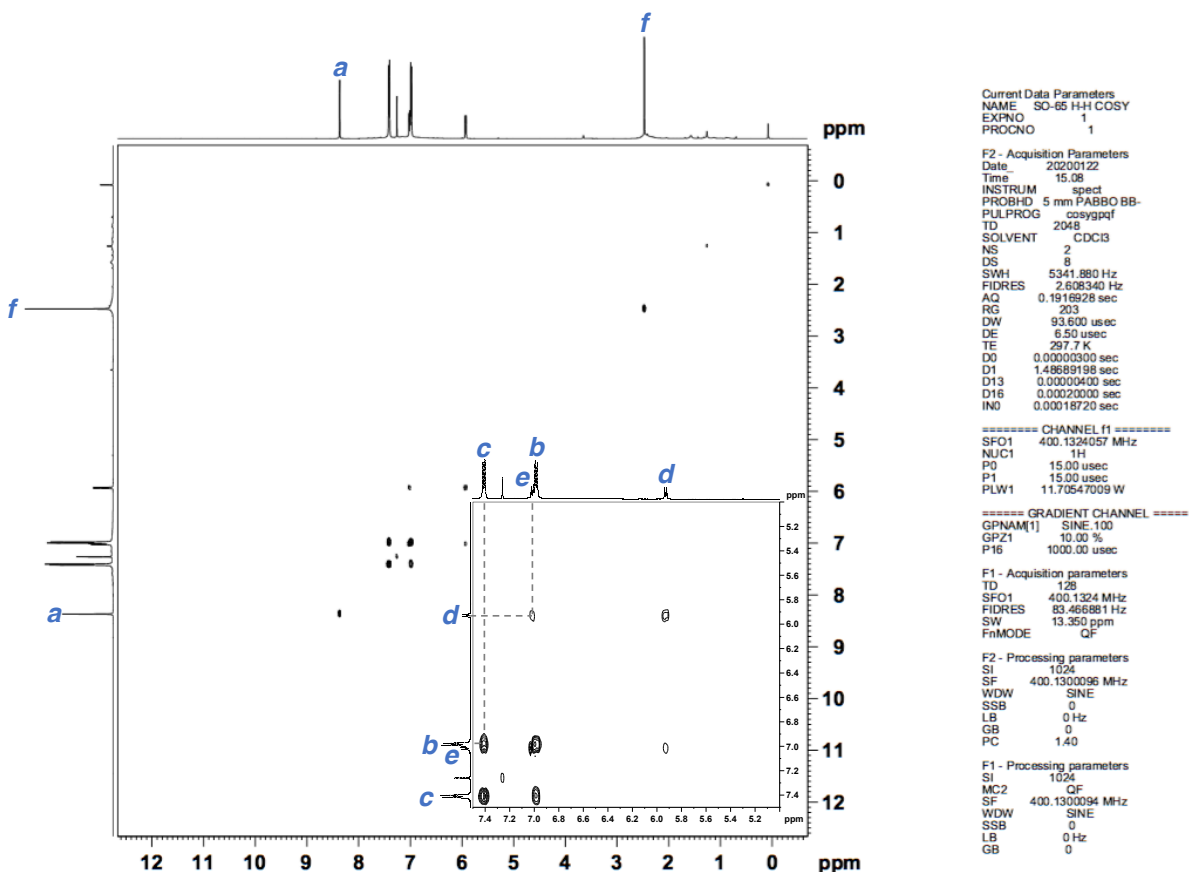


Figure S4d. A ¹H-H COSY NMR spectrum of **1CF₃** (500MHz, CDCl₃, r.t.).

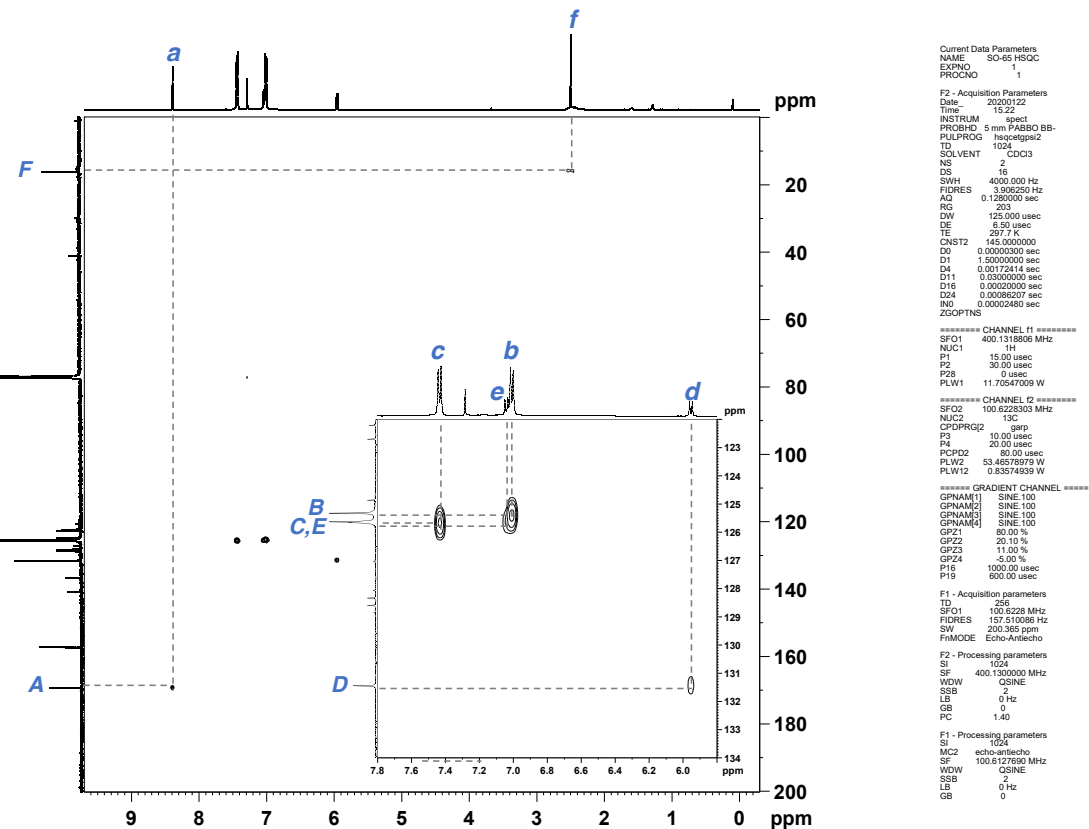


Figure S4e. A HSQC NMR spectrum of **1CF₃** (500MHz, CDCl₃, r.t.).

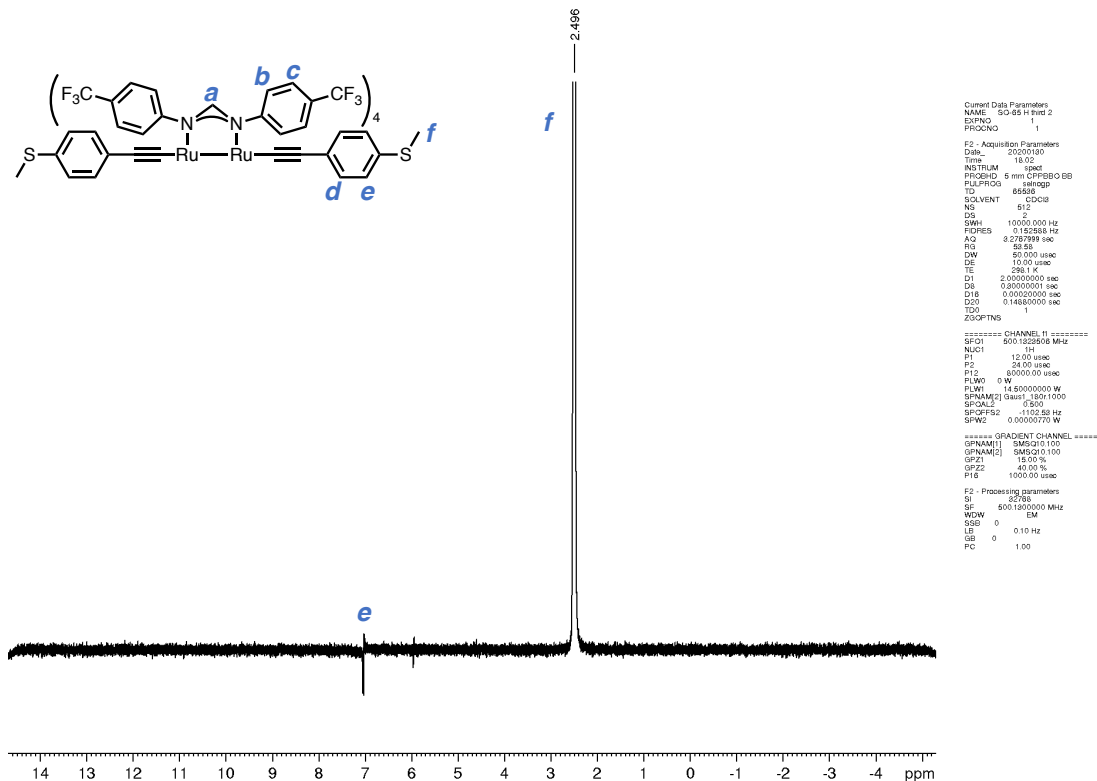


Figure S4f. A 1D NOESY NMR spectrum of **1^{CF3}** (500MHz, CDCl₃, r.t.).

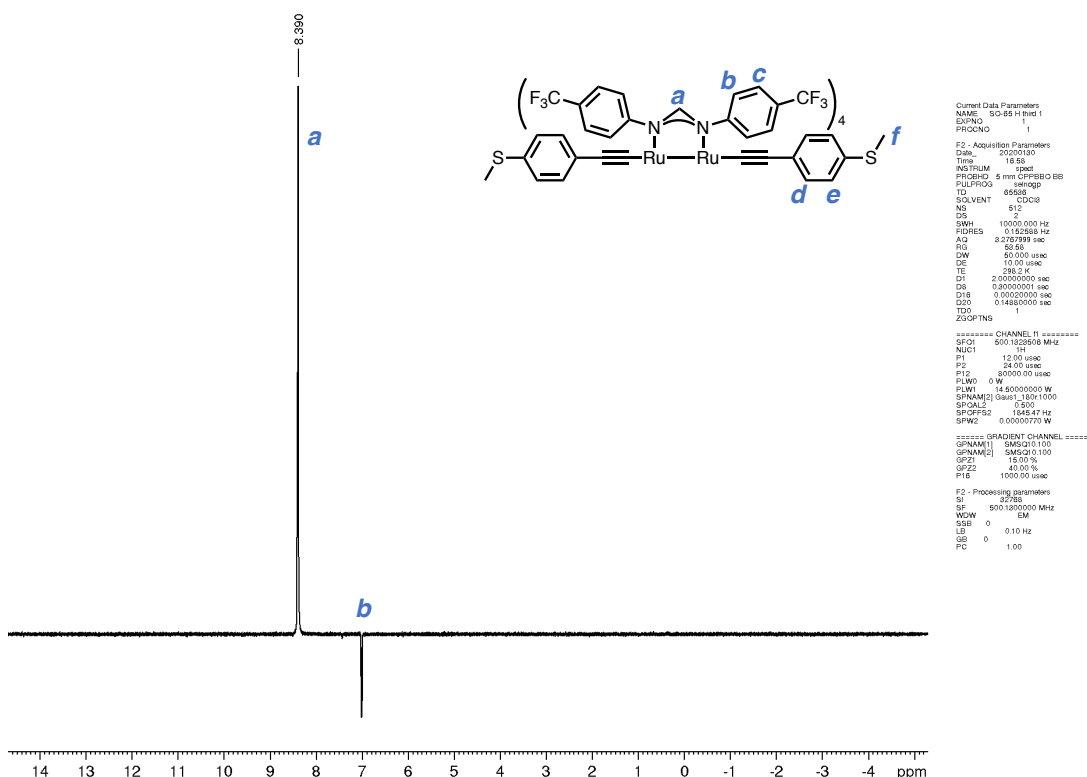


Figure S4g. A 1D NOESY NMR spectrum of **1^{CF3}** (500MHz, CDCl₃, r.t.).

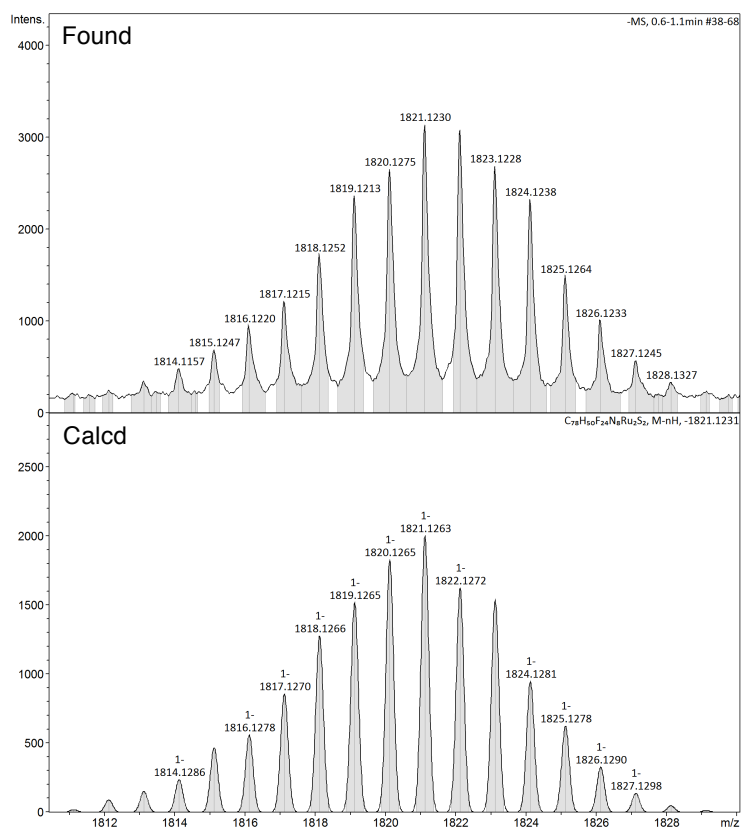


Figure S4h. HR-ESI-TOF-MS spectra of $\mathbf{1}^{\text{CF}_3}$ (MeOH).

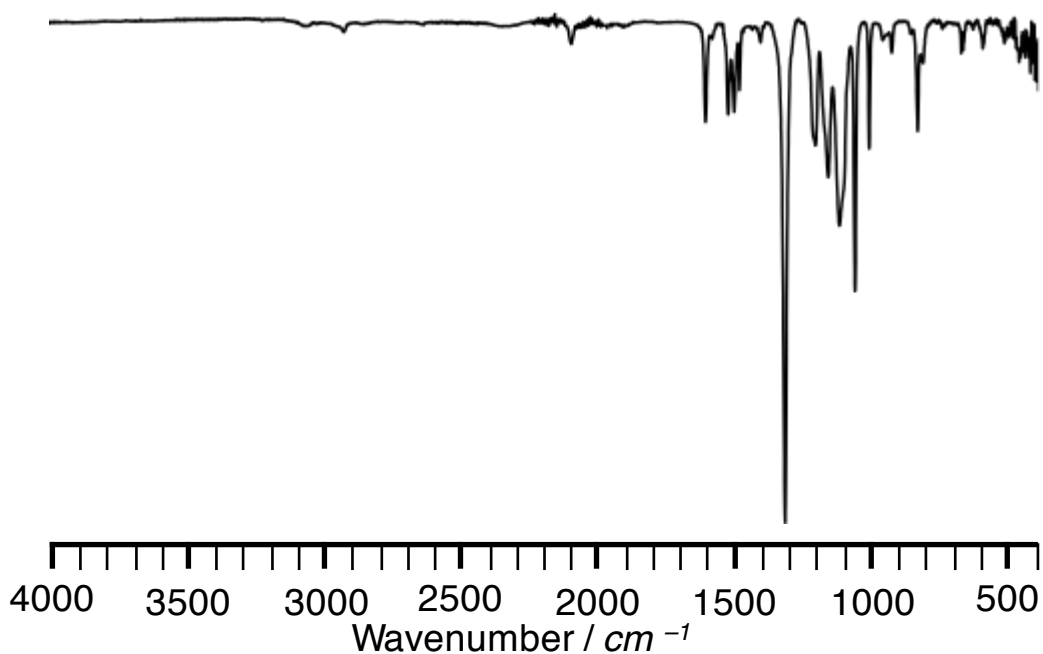
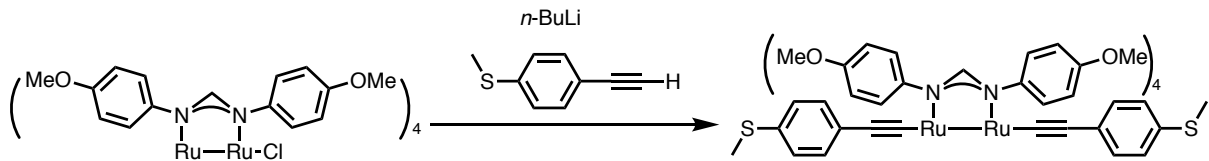


Figure S4i. An IR spectrum of $\mathbf{1}^{\text{CF}_3}$ (ATR, neat).



Synthesis of $\mathbf{1}^{\text{OMe}}$. The title complex was synthesized in a manner similar to that of $\mathbf{1}^{\text{H}}$ using 4-ethynylthioanisole (259 mg, 1.74 mmol, 110 equiv.), $n\text{-BuLi}$ (0.993 mL of a 1.6 M solution in $n\text{-hexane}$, 1.59 mmol, 100 equiv.), and $\mathbf{2}^{\text{OMe}}$ (20.0 mg, 0.0159 mmol, 1 equiv.), and was obtained as a dark purple solid in 49 % yield (11.9 mg, 0.00784 mmol).

^1H NMR: $\delta = 2.45$ (s, 6H, SMe), 3.69 (s, 24H, OMe), 6.29 (d, $J = 8.4$ Hz, 4H, $\text{C}_6\text{H}_4\text{SMe}$), 6.63 (d, $J = 8.8$ Hz, 16H, $\text{C}_6\text{H}_4\text{OMe}$), 6.80 (d, $J = 8.8$ Hz, 16H, $\text{C}_6\text{H}_4\text{OMe}$), 7.02 (d, $J = 8.4$ Hz, 4H, $\text{C}_6\text{H}_4\text{SMe}$), 8.17 (s, 4H, amidinate-H). $^{13}\text{C}\{\text{H}\}$ NMR: $\delta = 168.9$ (s, amidinate-C), 157.7 (s, C_{q}), 149.9 (s, C_{q}), 136.4 (s, C_{q}), 134.0 (s, C_{q}), 132.1 (s, $\text{C}_6\text{H}_4\text{SMe}$), 126.8 (q, $\text{C}_6\text{H}_4\text{OMe}$), 126.4 (s, $\text{C}_6\text{H}_4\text{OMe}$), 125.6 (s, C_{q}), 113.2 (s, $\text{C}_6\text{H}_4\text{OMe}$), 55.9 (s, OMe), 51.8 (s, C_{q}), 16.8 (s, SMe). HR-ESI-TOF-MS (MeOH) (m/z): Calcd. for $\text{C}_{78}\text{H}_{74}\text{N}_8\text{O}_8\text{Ru}_2\text{S}_2$: 1517.3118, Found 1517.3119 [$\text{M}-\text{H}]^-$. IR (ATR, neat / cm^{-1}): 1500 (s) 1585 (w), 1606 (m), 2085 (w) $\nu(\text{C}\equiv\text{C})$, 2836 (w), 2915 (w), 2933 (w), 2986 (m).

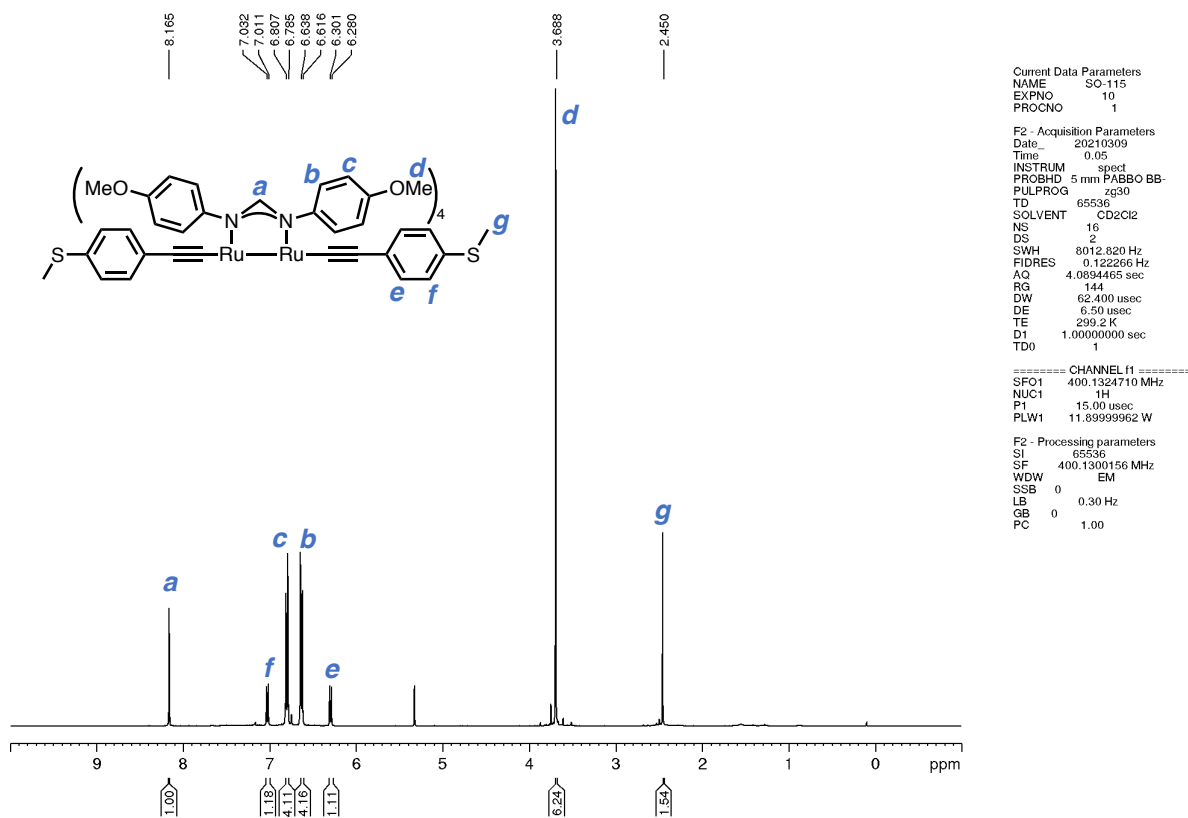


Figure S5a. A ^1H NMR spectrum of $\mathbf{1}^{\text{OMe}}$ (400MHz, CD_2Cl_2 , r.t.).

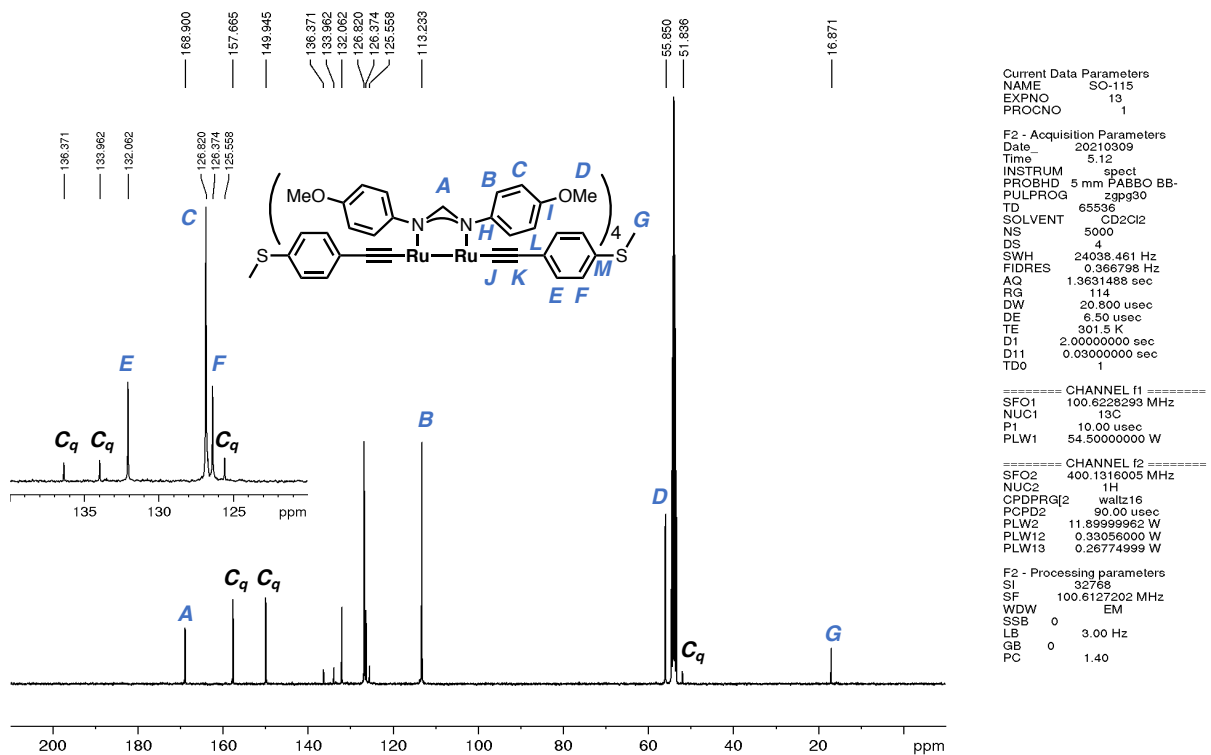


Figure S5b. A ¹³C{¹H} NMR spectrum of **1^{OMe}** (100 MHz, CD₂Cl₂, r.t.).

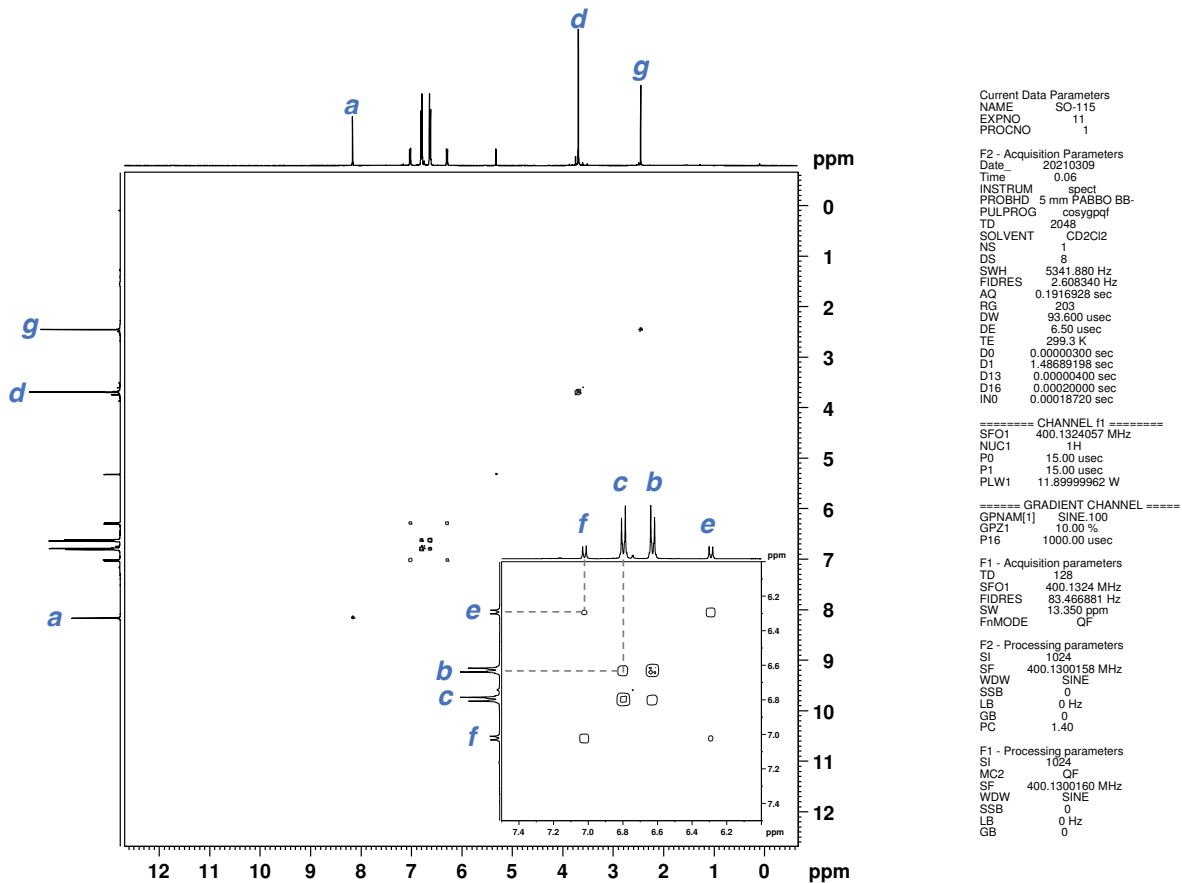


Figure S5c. A ¹H-H COSY NMR spectrum of **1^{OMe}** (400MHz, CDCl₃, r.t.).

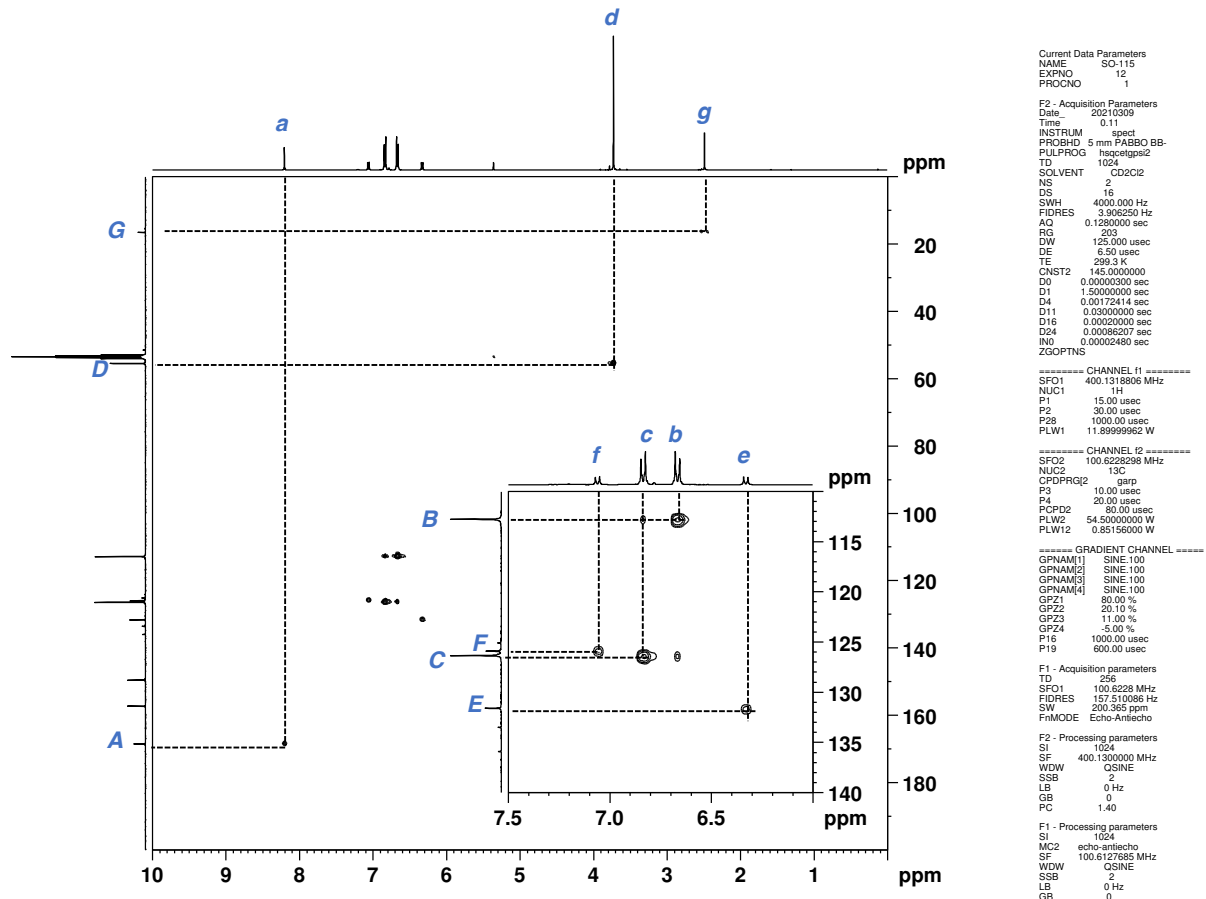


Figure S5d. A HSQC NMR spectrum of **1^{OMe}** (400MHz, CDCl₃, r.t.).

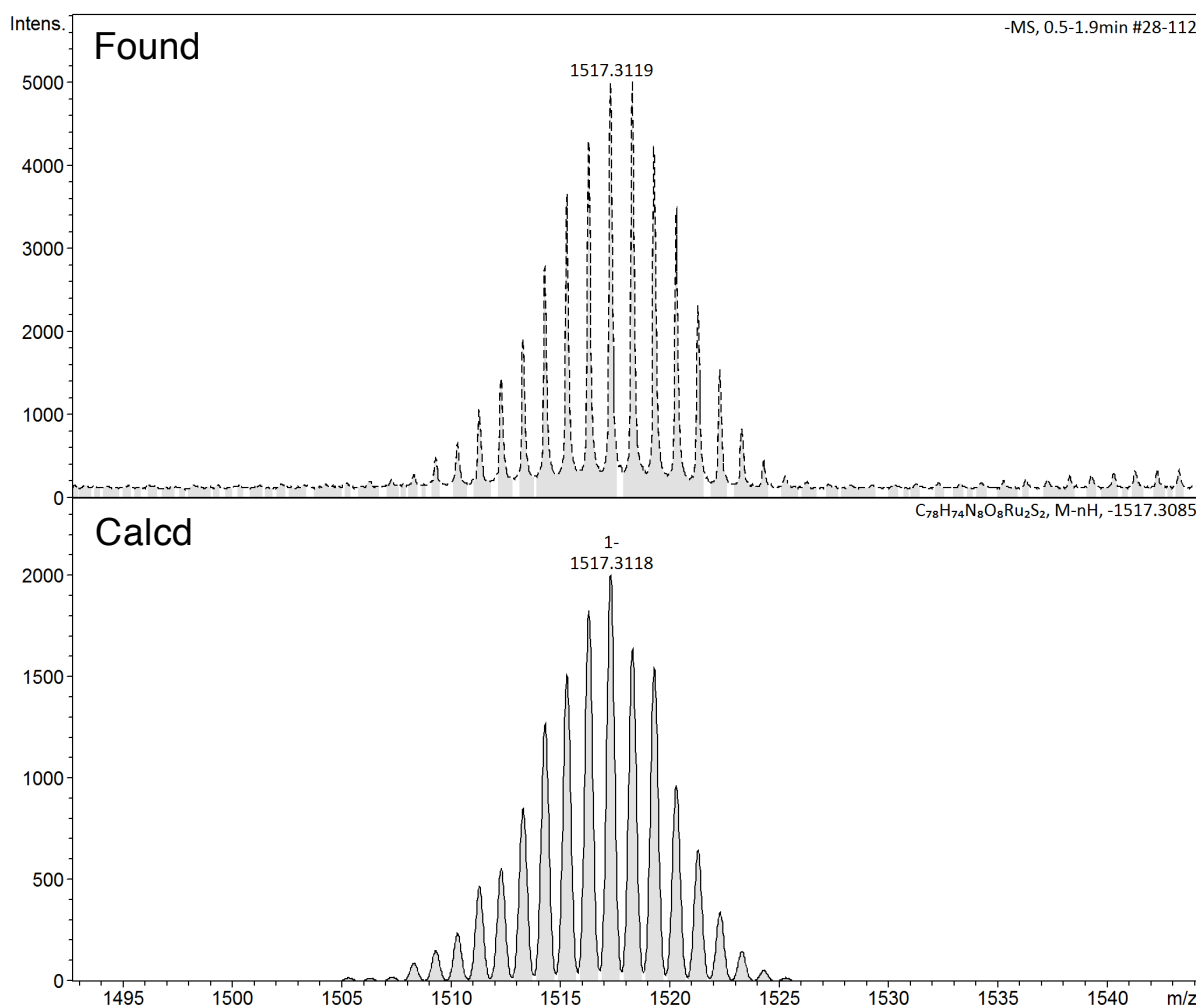


Figure S5e. HR-ESI-TOF-MS spectra of $\mathbf{1}^{\text{OMe}}$ (MeOH:CH₂Cl₂=1:1).

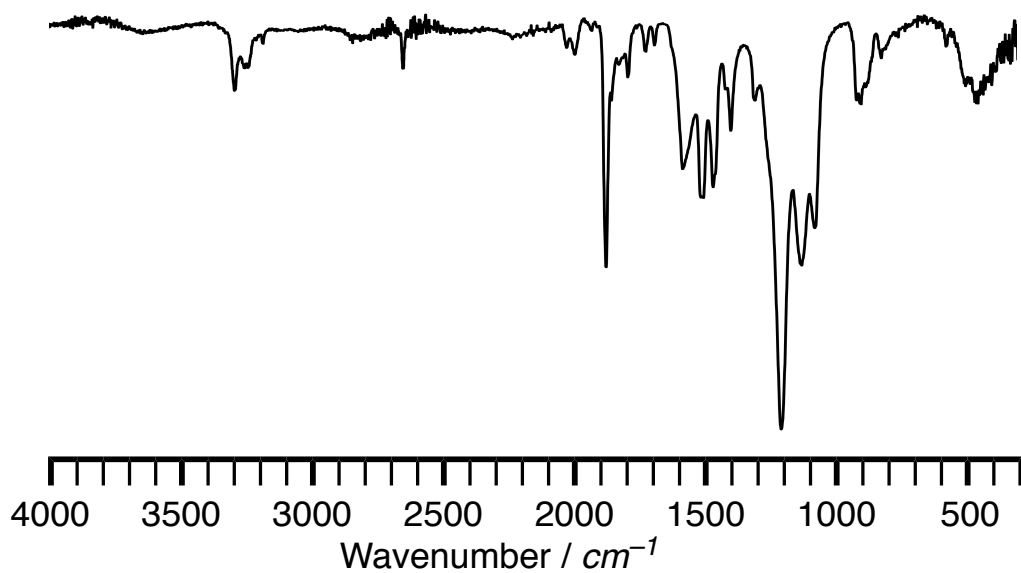


Figure S5f. An IR spectrum of $\mathbf{1}^{\text{OMe}}$ (ATR, neat).

III. STM-BJ

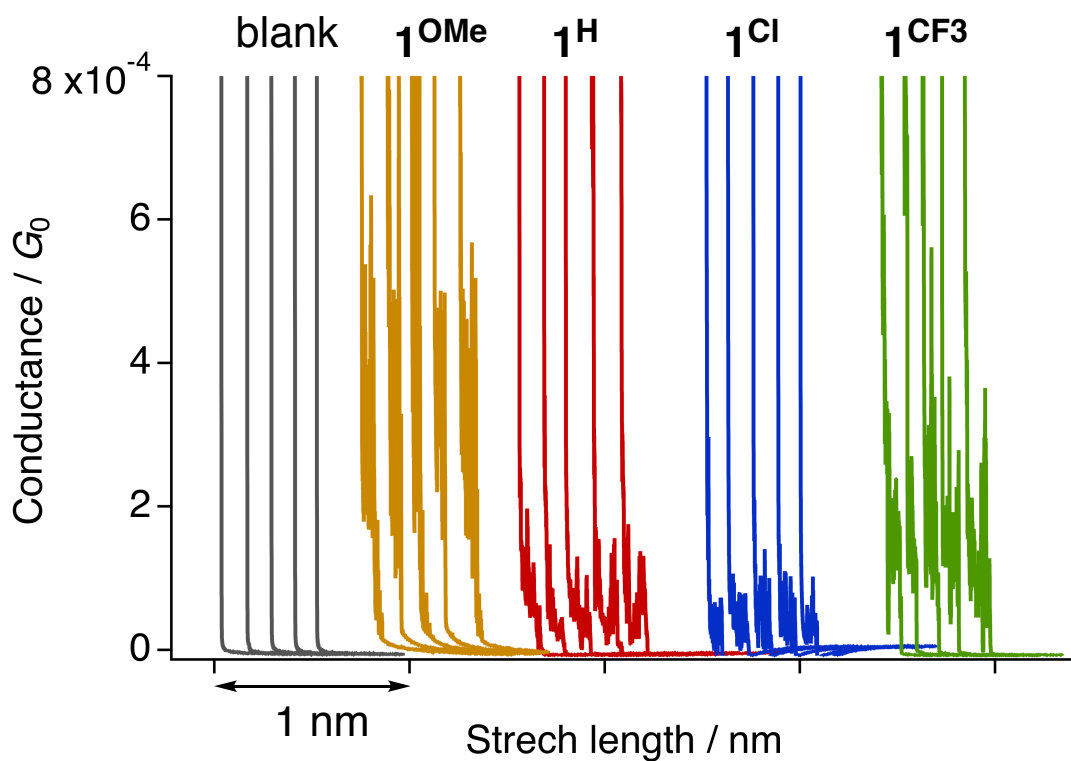


Figure S6. Typical individual traces for $\mathbf{1}^{\text{R}}$ ($\text{R} = \text{OMe}, \text{H}, \text{Cl}$, and CF_3).

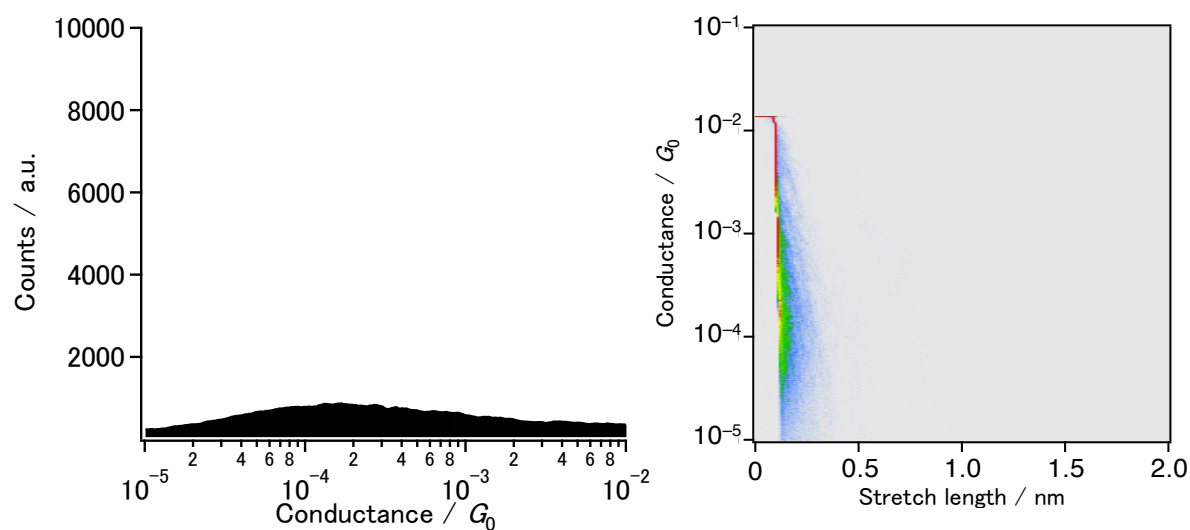


Figure S7. 1D and 2D log histograms of a tetraglyme solution (a blank experiment) constructed from 2000 traces without any data selection.

IV. X-ray Structures

Table S1. Crystal data and structure refinement for **1^R** ($\text{R}=\text{H}, \text{Cl}, \text{CF}_3$).

complex	1^H	1^{Cl}	1^{CF₃}
Empirical formula	$\text{C}_{70}\text{H}_{58}\text{N}_8\text{Ru}_2\text{S}_2$	$\text{C}_{70}\text{H}_{50}\text{Cl}_8\text{N}_8\text{Ru}_2\text{S}_2$	$\text{C}_{78}\text{H}_{50}\text{F}_{24}\text{N}_8\text{Ru}_2\text{S}_2$
Formula weight	1277.50	1553.04	1821.52
Temperature/K	93(2)	93(2)	90(2)
Crystal system	monoclinic	monoclinic	triclinic
Space group	C2/c	P2 ₁ /n	P-1
a/Å	24.1130(4)	14.9221(3)	12.3318(7)
b/Å	15.1675(3)	19.5861(4)	13.7567(8)
c/Å	16.6699(3)	23.0841(3)	15.6187(9)
$\alpha/^\circ$	90	90	68.497(5)
$\beta/^\circ$	104.800(2)	94.565(2)	86.771(4)
$\gamma/^\circ$	90	90	67.279(5)
Volume/Å ³	5894.48(19)	6725.3(2)	2262.7(2)
Z	4	4	1
$\rho_{\text{calc}}/\text{g/cm}^3$	1.440	1.534	1.337
μ/mm^{-1}	5.202	7.528	3.948
F(000)	2616.0	3128.0	910.0
Crystal size/mm ³	$0.20 \times 0.15 \times 0.15$	$0.30 \times 0.25 \times 0.25$	$0.20 \times 0.15 \times 0.10$
Radiation	Cu K α ($\lambda = 1.54184 \text{ \AA}$)	Cu K α ($\lambda = 1.54184 \text{ \AA}$)	Cu K α ($\lambda = 1.54184 \text{ \AA}$)
2 Θ range for data collection/°	6.952 to 149.64	6.814 to 149.946	7.514 to 149.764
Index ranges	-30 ≤ h ≤ 29, -17 ≤ k ≤ 18, -20 ≤ l ≤ 20	-18 ≤ h ≤ 18, -24 ≤ k ≤ 18, -28 ≤ l ≤ 27	-15 ≤ h ≤ 14, -16 ≤ k ≤ 14, -19 ≤ l ≤ 19
Reflections collected	28645	66360	25560
Independent reflections	5873 [R _{int} = 0.0354, R _{sigma} = 0.0209]	13475 [R _{int} = 0.0309, R _{sigma} = 0.0231]	8891 [R _{int} = 0.0427, R _{sigma} = 0.0420]
Data/restraints/parameters	5873/0/371	13475/1592/905	8891/863/526
Goodness-of-fit on F ²	1.065	1.037	1.326
Final R indexes [I>=2σ (I)]	R ₁ = 0.0307, wR ₂ = 0.0833	R ₁ = 0.0462, wR ₂ = 0.1196	R ₁ = 0.1068, wR ₂ = 0.2854
Final R indexes [all data]	R ₁ = 0.0314, wR ₂ = 0.0839	R ₁ = 0.0505, wR ₂ = 0.1228	R ₁ = 0.1125, wR ₂ = 0.2940
Largest diff. peak/hole / e Å ⁻³	0.66 / -0.89	1.96 / -1.09	5.06 / -1.24

V. Vis-NIR electronic spectral study

Vis-NIR absorption spectra of **1^R** recorded in CH₂Cl₂ are shown in Figure S8. The characteristics of the absorption bands for **1^R** ($R = \text{OMe}$, H, Cl, and CF₃) are similar with each other, i.e. with two bands located in the visible (400 - 700 nm) and NIR regions (800 - 1200 nm). The HOMO-LUMO gaps (Δ^{opt}) determined on the basis of the NIR absorption maxima (~950 nm) were ca. 1.3 eV, which are in good agreement with those obtained by the CV and DFT studies (see main text). We carried out TD-DFT calculations of **1^H** to assess character of the transitions. The computed Vis-NIR transitions were contributed by multiple orbitals. Thus we performed natural transition orbitals (NTOs) analysis of **1^H**^[11] and representative computed NIR transitions are shown in Figure S9. The three major computed NIR transitions are basically very similar to the transitions to LUMO from HOMO (transition A), HOMO-1 (transition B), and HOMO-2 (transition C). Thus, the transition character is a combination of the filled Ru₂ dπ*-to-vacant δ* transition (*d-d* transition) and the charge transfer (CT) transition from the axial thioanisylethynyl ligands to the Ru₂ core. On the other hand, the visible transition bands are also derived from the *d-d* transition but involve more significant contribution from the CT-type DArF and thioanisylethynyl ligands-to-Ru₂ core transitions (Figure S10).

The narrow HOMO-LUMO gaps of the Ru₂(DPhF)₄ dialkynyl complexes are fundamentally due to the weak ruthenium-ruthenium interaction as evidenced by the experimental and theoretical studies reported previously, i.e. the long Ru-Ru bond length.^[12,13] On the other hand, Δ^{opt} of Ru₂(DPhF)₄(C≡CPh)₂ was reported to be 1.78 eV, which is larger by 0.5 eV than those of **1^R**.^[12] The smaller Δ^{opt} values of **1^R** are, therefore, caused by the methylthio substituents on the phenyl groups, which raise the HOMO energies and enhance the CT character of the NIR transitions.

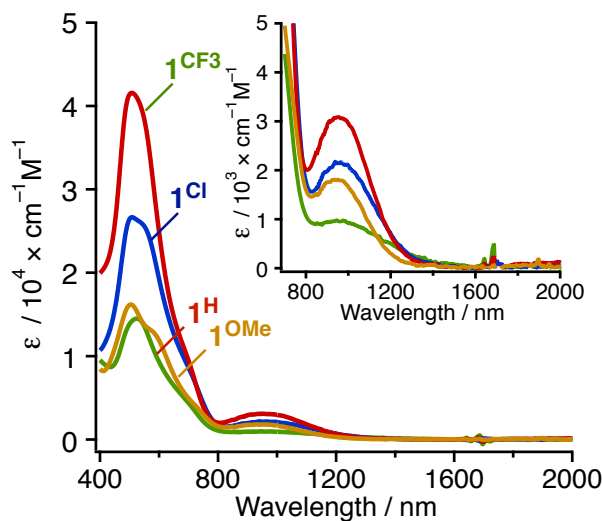


Figure S8. Vis-NIR spectra of **1^R** ($R = \text{OMe}$, H, Cl, and CF₃) recorded in CH₂Cl₂ (1 mM). Inset shows an expanded view of the NIR region.

V. DFT study

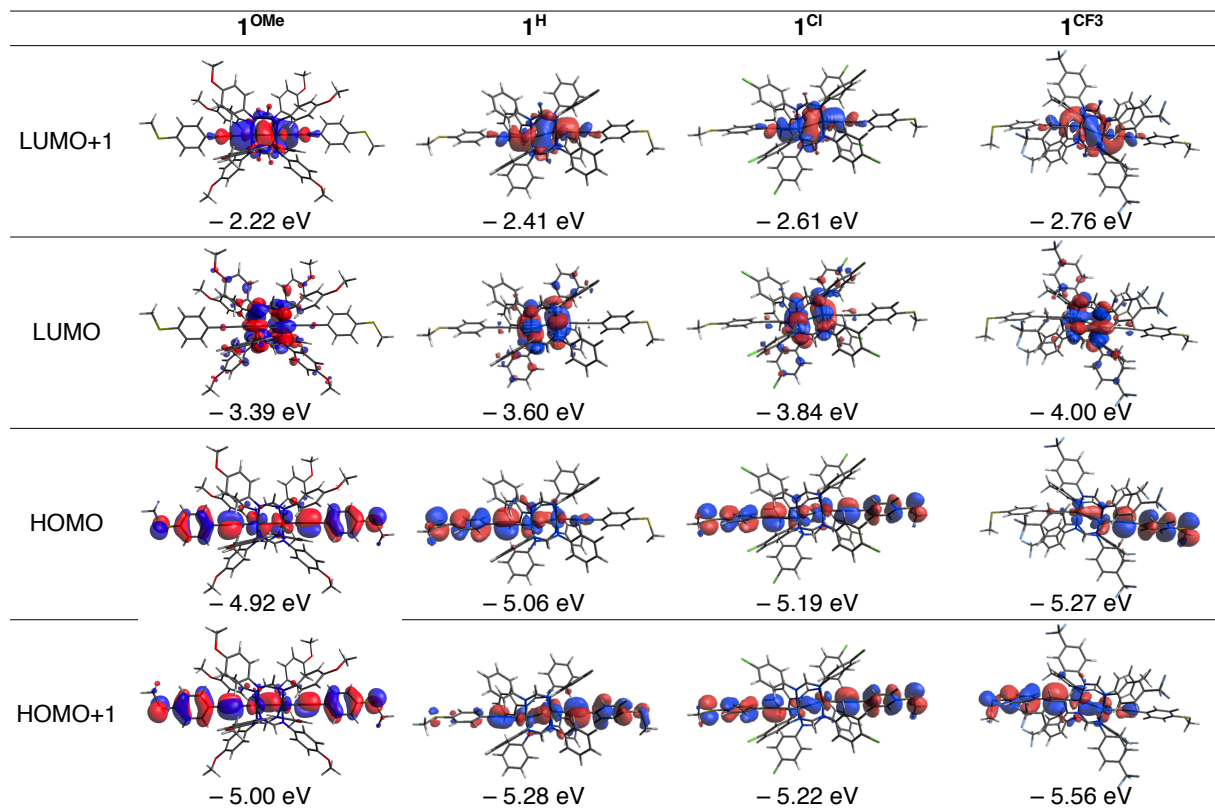


Figure S9. A part of Kohn-Sham orbitals of $\mathbf{1}^{\text{R}}$ ($\text{R} = \text{OMe}, \text{H}, \text{Cl}$, and CF_3).

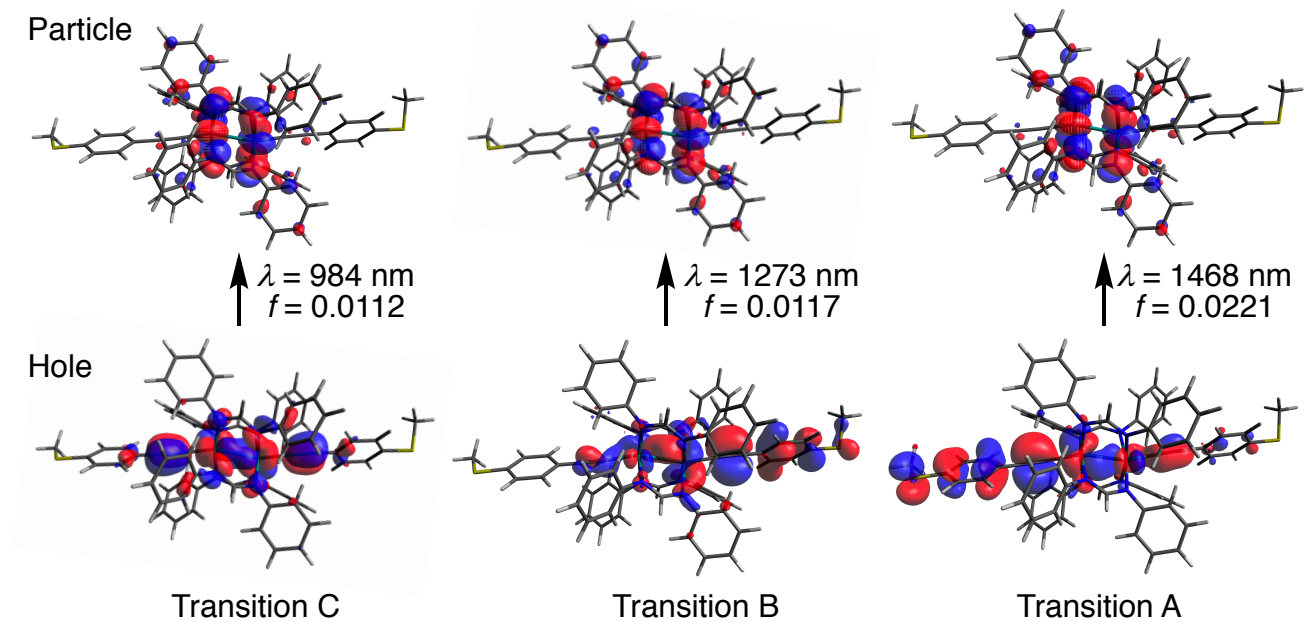


Figure S10. Hole-particle pairs of natural transition orbitals (NTOs) of $\mathbf{1}^{\text{H}}$ related to the NIR bands derived from the TD-DFT calculation. Hole-particle eigenvalues are near unity (~ 1.0) for these transitions.

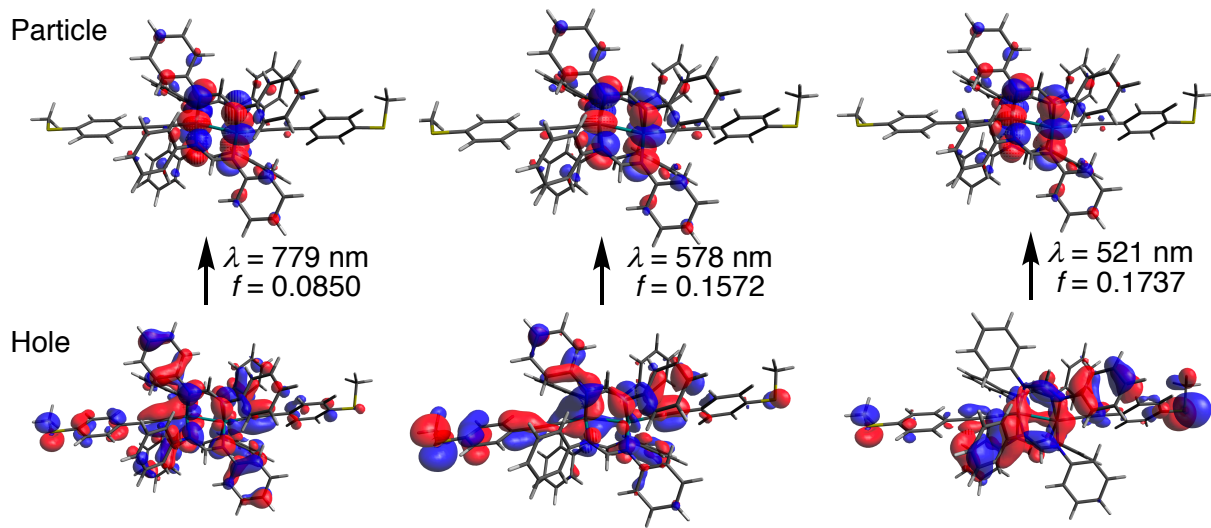


Figure S11. Hole–particle pairs of natural transition orbitals (NTOs) of $\mathbf{1}^{\text{H}}$ related to the visible transition bands derived from the TD-DFT calculation.

Table S2. TD-DFT data of $\mathbf{1}^{\text{OMe}}$.

$\lambda_{\max}^{\text{DFT}}$ nm	oscillator strength	main transition
1908.17	0.0000	HOMO → LUMO (71 %)
1364.38	0.0344	HOMO-1 → LUMO (89 %)
1318.18	0.0127	HOMO-2 → LUMO (67 %)
967.29	0.0402	HOMO-4 → LUMO (50 %)
898.19	0.0279	HOMO-3 → LUMO (99 %)
875.49	0.1030	HOMO-5 → LUMO (72 %)
778.33	0.1162	HOMO-4 → LUMO (41 %)
764.46	0.0089	HOMO → LUMO+1 (46 %)
682.93	0.0213	HOMO-8 → LUMO (62 %)
661.64	0.0419	HOMO-7 → LUMO (95 %)
649.56	0.0221	HOMO-9 → LUMO (43 %)
634.28	0.0151	HOMO-1 → LUMO+1 (38 %)
631.16	0.0036	HOMO-1 → LUMO+1 (48 %)
604.23	0.1968	HOMO-12 → LUMO (37 %)
575.89	0.0261	HOMO-11 → LUMO (75 %)
574.64	0.1212	HOMO-14 → LUMO (36 %)
560.38	0.0056	HOMO-4 → LUMO+1 (42 %)
548.67	0.0069	HOMO-3 → LUMO+1 (45 %)
531.45	0.0015	HOMO-13 → LUMO (33 %)
511.58	0.0310	HOMO-5 → LUMO+1 (66 %)

Table S3. TD-DFT data of **1^H**.

$\lambda_{\max}^{\text{DFT}}$ nm	oscillator strength	main transition
2021.49	0.0009	HOMO → LUMO (51 %)
1468.03	0.0221	HOMO–1 → LUMO (40 %)
1273.28	0.0117	HOMO–2 → LUMO (68 %)
984.23	0.0112	HOMO–4 → LUMO (62 %)
799.4	0.0385	HOMO–3 → LUMO (80 %)
779.64	0.085	HOMO–5 → LUMO (82 %)
769.09	0.0111	HOMO → LUMO+1 (39 %)
687.07	0.0755	HOMO–6 → LUMO (68 %)
654.31	0.0304	HOMO–7 → LUMO (44 %)
632.81	0.0212	HOMO–1 → LUMO+1 (40 %)
586.44	0.1572	HOMO–9 → LUMO (35 %)
559.02	0.0372	HOMO–4 → LUMO+1 (35 %)
546.3	0.0099	HOMO–10 → LUMO (73 %)
544.79	0.0287	HOMO–4 → LUMO+1 (30 %)
534.37	0.0278	HOMO–11 → LUMO (52 %)
532.43	0.0038	HOMO–3 → LUMO+1 (46 %)
520.95	0.1737	HOMO–8 → LUMO (36 %)
514.33	0.0238	HOMO–12 → LUMO (83 %)
487.58	0.0117	HOMO–13 → LUMO (75 %)
480.13	0.0002	HOMO–3 → LUMO+1 (33 %)

Table S4. TD-DFT data of **1^{Cl}**.

$\lambda_{\max}^{\text{DFT}}$ nm	oscillator strength	main transition
2212.05	0.0001	HOMO → LUMO (60 %)
1703.45	0.0454	HOMO–1 → LUMO (92 %)
1549.61	0.0031	HOMO–2 → LUMO (62 %)
1010.58	0.013	HOMO–5 → LUMO (67 %)
830.17	0.0925	HOMO–4 → LUMO (85 %)
821.61	0.046	HOMO–3 → LUMO (84 %)
775.19	0.0059	HOMO → LUMO+1 (45 %)
710.84	0.1089	HOMO–6 → LUMO (62 %)
678.89	0.003	HOMO–7 → LUMO (49 %)
671.3	0.0006	HOMO–1 → LUMO+1 (86 %)
629.44	0.214	HOMO–8 → LUMO (32 %)
602.76	0.0509	HOMO–9 → LUMO (80 %)
572.68	0.0079	HOMO–10 → LUMO (88 %)
564.99	0.0327	HOMO–11 → LUMO (59 %)
549.4	0.0012	HOMO–5 → LUMO+1 (55 %)
546.15	0.1793	HOMO–11 → LUMO (27 %)
540.28	0.0337	HOMO–12 → LUMO (63 %)
528.25	0.0056	HOMO–3 → LUMO+1 (54 %)
508.19	0.0245	HOMO–13 → LUMO (66 %)
492.29	0.0046	HOMO–14 → LUMO (84 %)

Table S5. TD-DFT data of **1^{CF3}**.

$\lambda_{\max}^{\text{DFT}}$ nm	oscillator strength	main transition
2272.8	0.0041	HOMO → LUMO (43 %)
1775.05	0.0264	HOMO → LUMO (49 %)
1471.71	0.0118	HOMO–1 → LUMO (53 %)
1031.23	0.0081	HOMO–3 → LUMO (60 %)
795.05	0.0759	HOMO–5 → LUMO (62 %)
789.68	0.05	HOMO–4 → LUMO (41 %)
772.71	0.0107	HOMO–2 → LUMO+1 (37 %)
689.26	0.033	HOMO–7 → LUMO (36 %)
671.48	0.0644	HOMO–9 → LUMO (25 %)
660.73	0.0387	HOMO–1 → LUMO+1 (27 %)
623.34	0.0904	HOMO–6 → LUMO (40 %)
618.2	0.0609	HOMO–8 → LUMO (41 %)
561.62	0.1482	HOMO–9 → LUMO (20 %)
548.04	0.0279	HOMO–4 → LUMO+1 (34 %)
538.74	0.0095	HOMO–12 → LUMO (75 %)
526.23	0.0015	HOMO–3 → LUMO+1 (32 %)
515.48	0.0926	HOMO–13 → LUMO (64 %)
501.75	0.0464	HOMO–14 → LUMO (79 %)
486.77	0.0026	HOMO–10 → LUMO (49 %)
482.13	0.0029	HOMO–10 → LUMO (31 %)

IV. DFT-NEGF study

(1) TranSIESTA

Electronic transport properties were simulated by using the TranSIESTA code.^[14] We employed the Perdew-Burke-Ernzerhof exchange-correlation functional,^[15] the single- ζ plus polarization basis set for Au atoms, the double- ζ plus polarization basis set for molecular atoms, and a cutoff energy of 300 Ry for the real-space integrations. An Au(111)-p(6x6) slab was employed as the electrodes and the bottom three layers were treated as the self-energies. Molecular geometries were optimized with Gaussian 16(C1) program package as described above. Because the surface area of the cell is large, only gamma point was sampled for calculating the electronic structure and the transmission function by the post processing TBTrans tool. The transmission eigenchannels^[16] at the Fermi level were visualized using the Inelastica package.

(2) Level-broadening approach based on the NEGF and hybrid DFT method.^[17]

DFT calculations for electron transport were performed by using the Gaussian 09 (D01) program package^[18] and the non-equilibrium Green's function (NEGF) method in a level-broadening approach.^{[17][19]} B3LYP/LanL2DZ (for Ru and Au) and 6-31G(d) (for C, H, N, S, Cl, F) levels of theory were adopted for the transport calculations.

The computational procedure in the level-broadening approach is as follows.

- I. Structural optimization of cluster models for Au-molecule-Au junctions.
- II. Determination of the cluster sizes and scattering regions.
- III. Calculations of transmission functions with the NEGF method.

In Step I (structural optimization), a molecular junction model, in which a molecule is sandwiched between Au_x clusters were constructed. Because we sometimes meet computational difficulties in structural relaxations, geometry optimization of the molecular junction models were performed in a stepwise manner. First, we carried out geometry optimization of molecules with the edge single Au atoms (e.g., Au_1 -molecule- Au_1). Then, we expanded the edge Au atoms to trigonal pyramid Au_{10} clusters (Au_{10} -molecule- Au_{10}). During the second optimization process, the third Au layers (Au_6) were frozen, while the Au_4 clusters were relaxed. Finally, the molecular junction model was expanded to Au_{35} -molecule- Au_{35} , and the models were used for the next steps.

Step II is related to the computational procedure in transmission calculations in Step III, and thus we firstly introduce the essence of the NEGF method with the broadening approach.

- 1) The cluster model for a molecular junction is composed of a left metal cluster, a sandwiched molecule and

a right metal cluster (Figure. S1).

- 2) The sandwiched molecule and 4 gold atoms in both clusters are defined as an extended molecule (Figure. S1).
- 3) Metal cluster atoms except for the metal atoms in the EM region are recognized as electrode clusters, and the density of states of the metal clusters are broadened (i.e., level-broadening) to obtain Green's functions of the metal clusters.
- 4) Broadening parameters for the metal clusters are chosen so as to show a reasonable conductance in a reference system (e.g., $2e^2/h$ in a one-dimensional gold chain).
- 5) The size of the metal cluster and EM region are determined to hold the condition that the calculated conductance is almost insensitive to those sizes.
- 6) When the Fermi energy was set to -5.18 eV, the experimental results were well reproduced.

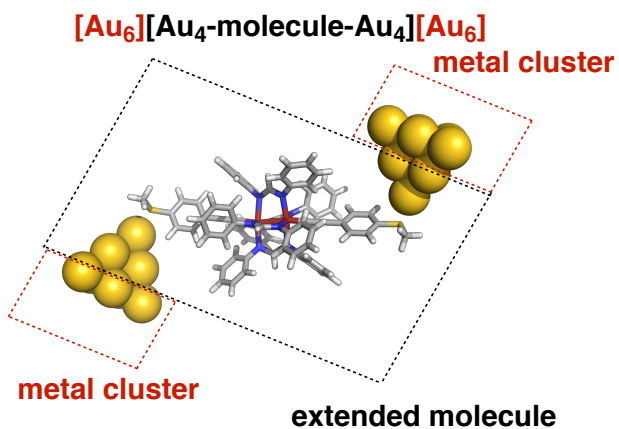


Figure S12. Model definition in a level-broadening approach.

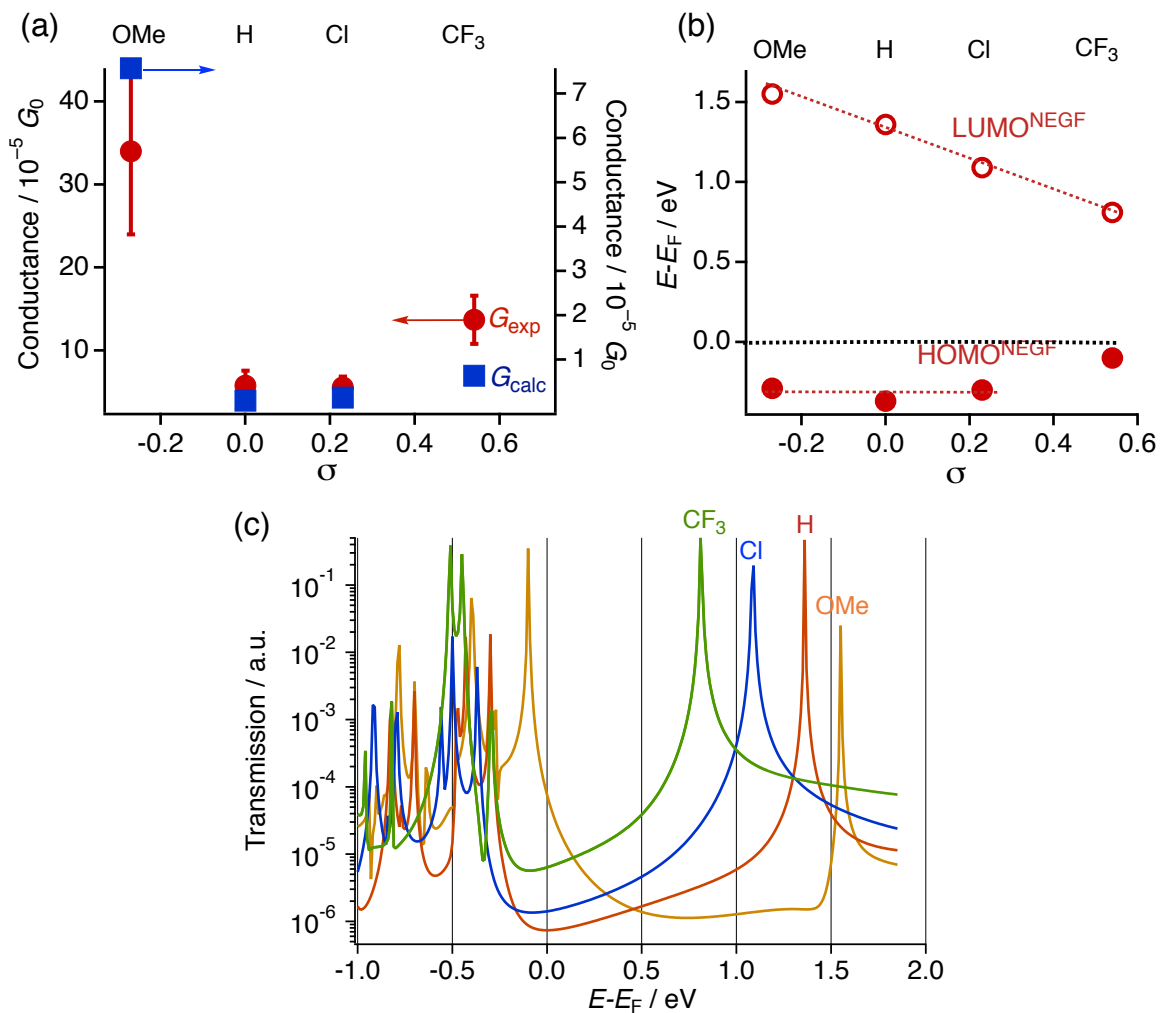


Figure S13. Plots of (a) experimentally (G_{exp}) and theoretically obtained conductance (G_{calc}) and (b) HOMO^{NEGF} and LUMO^{NEGF} against Hammett substituent constants σ . (c) Transmission spectra of of $\text{Au}_{10}\text{-R-Au}_{10}$ (R = OMe, H, Cl, and CF₃).

Table S6. Cartesian coordinates of **1^{OMe}** ($E = -5040.65491733$ hartree).

C	8.71845	-0.46889	-0.48102	C	-6.60897	1.21222	-0.80156
C	8.06877	-0.18248	0.72762	C	-5.89686	0.32566	0.03245
C	6.67921	-0.07481	0.77245	C	-6.64809	-0.44474	0.95071
C	5.88639	-0.24637	-0.38183	C	-8.03056	-0.33124	1.02752
C	6.55848	-0.53241	-1.59267	C	-8.72532	0.55971	0.19019
C	7.94267	-0.64231	-1.64079	C	-7.99644	1.33041	-0.72585
S	10.48724	-0.63124	-0.66416	S	-10.50014	0.62175	0.37715
C	11.13102	-0.34442	1.01795	C	-11.02668	1.87172	-0.84211
C	4.20151	-0.61253	-4.9548	H	0.21047	-3.22072	1.8213
C	3.56459	0.58056	-4.58713	H	-0.27536	3.29865	-1.96639
C	2.55829	0.56164	-3.61823	H	-3.51933	-2.74175	0.22732
C	2.16934	-0.63141	-3.00412	H	-5.22999	-3.92339	1.58396
C	2.81357	-1.82186	-3.37786	H	-2.72187	-3.5463	5.0614
C	3.81807	-1.81444	-4.33901	H	-1.04283	-2.3697	3.71757
N	1.09949	-0.63478	-2.04582	H	-3.04928	-0.14937	3.07481
C	0.06709	-1.3745	-2.42078	H	-4.9476	0.91426	4.21999
N	-1.10013	-1.47064	-1.77041	H	-3.72774	4.74452	2.68203
C	-1.96705	-2.51109	-2.21084	H	-1.79937	3.65632	1.54446
C	-1.47366	-3.7982	-2.47154	H	-2.22401	0.27616	-3.55327
C	-2.31221	-4.82172	-2.92049	H	-4.05578	1.05904	-4.99324
C	-3.67559	-4.56824	-3.11301	H	-4.46265	4.5798	-2.54973
C	-4.17977	-3.2843	-2.84341	H	-2.61591	3.7732	-1.09707
C	-3.34118	-2.2724	-2.39694	H	-0.42366	-4.01783	-2.30277
Ru	-1.3089	-0.2182	-0.16673	H	-1.89268	-5.80408	-3.1028
Ru	1.29782	0.25063	-0.09957	H	-5.23925	-3.09952	-2.99376
N	1.03878	2.12667	-0.87135	H	-3.74135	-1.2905	-2.17802
C	1.89824	3.25825	-0.77574	H	3.65701	2.20448	-1.4361
C	1.40928	4.49813	-0.33844	H	5.13875	4.19682	-1.30788
C	2.23935	5.61896	-0.25415	H	1.82411	6.55654	0.09643
C	3.58965	5.5108	-0.60793	H	0.3704	4.5913	-0.03636
C	4.08945	4.26951	-1.03786	H	0.15749	-1.93792	-3.35183
C	3.2594	3.15995	-1.11817	H	2.53719	-2.75542	-2.8967
N	-1.14458	-1.83617	1.09248	H	4.32121	-2.73289	-4.62578
C	-2.1447	-2.48584	1.86727	H	3.83441	1.52337	-5.04856
C	-3.34865	-2.9175	1.28159	H	2.06493	1.48657	-3.34222
C	-4.3071	-3.57652	2.03927	H	1.79808	-3.96561	-0.53448
C	-4.09899	-3.82008	3.40807	H	3.75866	-5.45592	-0.17033
C	-2.91071	-3.38679	4.00625	H	5.11283	-2.85874	2.9833
C	-1.94968	-2.72425	3.23596	H	3.18212	-1.38533	2.59803
N	-1.16237	1.06387	1.58075	H	-0.10809	1.86592	3.17029
C	-0.0307	1.33693	2.21758	H	1.22112	0.20188	4.3435
N	1.20147	1.03878	1.79726	H	2.9708	0.57974	6.01904
C	2.24062	1.23432	2.74829	H	5.32449	2.66439	3.0795
C	3.42094	1.91641	2.40138	H	3.54222	2.28864	1.39232
C	4.41919	2.1256	3.34304	H	-6.12899	-1.13901	1.60461
C	4.27514	1.65551	4.66003	H	-6.06223	1.8188	-1.51735
C	3.11046	0.96698	5.01651	H	-8.57785	-0.93934	1.74391
C	2.10921	0.76057	4.06212	H	-8.49721	2.02801	-1.3883

N	-1.17872	1.51159	-1.43424	H	6.19262	0.15041	1.71677
C	-2.28396	1.96651	-2.23046	H	5.97826	-0.67046	-2.49998
C	-2.71347	1.21678	-3.32842	H	8.63338	-0.03973	1.64257
C	-3.75504	1.66332	-4.14528	H	8.42804	-0.86457	-2.58813
C	-4.38754	2.8823	-3.86558	H	12.21678	-0.43652	0.93689
C	-3.96334	3.63927	-2.76205	H	10.88469	0.65882	1.37465
C	-2.92377	3.18641	-1.95745	H	10.76175	-1.09557	1.72068
C	0.10032	-2.29068	1.25885	H	-12.11348	1.9344	-0.7483
N	1.20839	-1.72715	0.79452	H	-10.59347	2.85082	-0.62287
C	2.36223	-2.56292	1.00091	H	-10.7746	1.56752	-1.86108
C	3.30584	-2.27359	1.98907	C	-3.25726	0.06899	-0.07622
C	4.40214	-3.11192	2.20507	C	-4.47638	0.20857	-0.03773
C	4.57233	-4.25856	1.41763	C	3.24574	-0.01834	-0.24061
C	3.62449	-4.56051	0.42916	C	4.46476	-0.13711	-0.32474
C	2.53088	-3.72306	0.22993	O	4.48992	6.53291	-0.56382
C	-2.29886	1.67256	2.22188	O	5.31585	1.91602	5.50321
C	-3.19552	0.92103	2.98461	O	5.19229	-0.71006	-5.88842
C	-4.27351	1.52776	3.63349	O	5.61149	-5.13757	1.53864
C	-4.47268	2.90994	3.51675	O	-4.58448	-5.48717	-3.54493
C	-3.57175	3.67268	2.7596	O	-5.10458	-4.47541	4.05677
C	-2.49569	3.05841	2.12565	O	-5.41099	3.41353	-4.59582
C	-0.15425	2.35099	-1.43742	O	-5.49759	3.59959	4.10077
C	6.628	-4.84739	2.49189	H	3.2506	8.20194	-0.78853
H	7.36216	-5.64955	2.4004	C	-6.46663	2.86305	4.83899
H	7.1111	-3.88519	2.28092	H	-7.19748	3.59475	5.18721
H	6.22971	-4.83564	3.51417	H	-6.9682	2.11826	4.20861
C	5.62541	0.48113	-6.53776	H	-6.01661	2.36036	5.70423
H	6.41359	0.17567	-7.22761	C	5.21559	1.47113	6.85214
H	4.8096	0.94947	-7.10214	H	5.13173	0.37875	6.90857
H	6.0307	1.20434	-5.81938	H	6.13757	1.78891	7.34144
C	-4.12647	-6.80502	-3.83349	H	4.35733	1.92674	7.3613
H	-3.70459	-7.28593	-2.94251	C	-4.93914	-4.75735	5.44272
H	-5.00527	-7.36103	-4.16324	H	-4.83897	-3.83612	6.02995
H	-3.37619	-6.80116	-4.63361	H	-5.84263	-5.28596	5.75044
C	-5.88505	2.68201	-5.72197	H	-4.06517	-5.3963	5.61981
H	-6.69352	3.27875	-6.1471	C	4.0372	7.81242	-0.1308
H	-5.09753	2.54865	-6.47391	H	3.6638	7.77659	0.89994
H	-6.27405	1.69972	-5.42675	H	4.9073	8.46882	-0.17824

Table S8. Cartesian coordinates of **1^H** ($E = -4124.45439704$ hartree).

C	-8.73627	0.24822	-0.22263	C	2.38917	-2.14302	1.67725
C	-8.05637	-0.32858	0.85908	C	3.27707	-1.60134	2.61475
C	-6.66313	-0.379	0.86978	C	4.36994	-2.3491	3.05433
C	-5.8972	0.14044	-0.19456	C	4.59456	-3.63781	2.56003
C	-6.59823	0.71617	-1.27918	C	3.70905	-4.18046	1.6271
C	-7.98638	0.76949	-1.29205	C	2.60752	-3.43886	1.19141
S	-10.51203	0.37411	-0.34878	H	5.44861	-4.21451	2.90403
C	-11.11786	-0.40924	1.18252	C	0.1917	-1.83316	-1.99451

H	-5.09963	2.06173	-5.19724	C	6.62559	-0.61352	-1.1705
C	-4.30477	1.87778	-4.48005	C	5.90617	-0.05628	-0.08838
C	-3.6217	0.65771	-4.48302	C	6.64517	0.44907	1.00436
C	-2.59844	0.41827	-3.56503	C	8.0367	0.39109	1.01851
C	-2.24635	1.4016	-2.63194	C	8.73829	-0.16552	-0.06042
C	-2.93028	2.6252	-2.62989	C	8.01627	-0.65835	-1.15852
C	-3.95485	2.85931	-3.54937	S	10.53311	-0.18586	-0.05048
N	-1.15765	1.16509	-1.72341	C	10.87855	-1.97376	0.18938
C	-0.15069	2.00938	-1.8885	H	-0.26461	2.58256	2.70199
N	1.02782	1.94811	-1.25578	H	0.33163	-2.59351	-2.76554
C	1.86426	3.09379	-1.40052	H	3.4126	2.72784	0.96242
C	1.33273	4.38477	-1.23387	H	5.12405	3.55504	2.54822
C	2.14654	5.50839	-1.38641	H	2.76725	2.11076	5.84689
C	3.49886	5.36118	-1.70179	H	1.06748	1.27247	4.25775
C	4.03156	4.0781	-1.86028	H	3.10195	-0.60255	2.99784
C	3.22597	2.94932	-1.70931	H	5.04868	-1.92199	3.7878
H	4.13255	6.2357	-1.81773	H	3.86699	-5.18379	1.24065
Ru	1.30042	0.3097	-0.06262	H	1.91072	-3.86131	0.4731
Ru	-1.29234	-0.2371	-0.10607	H	2.11452	0.77966	-3.51704
N	-0.99966	-1.80724	-1.38319	H	3.96351	0.4547	-5.13827
C	-1.83033	-2.94499	-1.60375	H	4.56674	-3.53388	-3.63668
C	-1.29705	-4.24234	-1.5067	H	2.72675	-3.1941	-2.01066
C	-2.10546	-5.35698	-1.73516	H	0.28839	4.50573	-0.96196
C	-3.45429	-5.19457	-2.05782	H	1.72095	6.49849	-1.24851
C	-3.98903	-3.90561	-2.14657	H	5.08261	3.95214	-2.10575
C	-3.18886	-2.78578	-1.91962	H	3.64061	1.95556	-1.81951
H	-4.08389	-6.06224	-2.23271	H	-3.6054	-1.78819	-1.97431
N	1.11514	1.50754	1.5948	H	-5.03755	-3.76794	-2.39656
C	2.11565	1.9617	2.49961	H	-1.67856	-6.3525	-1.65061
C	3.27659	2.59388	2.02778	H	-0.25562	-4.37686	-1.23011
C	4.23661	3.05581	2.92795	H	-0.27453	2.81089	-2.61944
C	4.06233	2.89096	4.30614	H	-2.66995	3.38287	-1.89696
C	2.91345	2.25512	4.77993	H	-4.47968	3.81065	-3.53479
C	1.94699	1.79008	3.88555	H	-3.88023	-0.10972	-5.20758
H	4.8149	3.25293	5.00077	H	-2.06249	-0.52379	-3.57161
N	1.2242	-1.41272	1.2488	H	-1.96092	3.86558	0.62033
C	0.1127	-1.8971	1.78832	H	-3.9345	5.13327	1.436
N	-1.13492	-1.53059	1.48288	H	-5.06122	1.77179	3.87608
C	-2.15119	-2.03354	2.34335	H	-3.09774	0.50764	3.03698
C	-3.31135	-2.62226	1.81673	H	0.22295	-2.6776	2.54401
C	-4.28865	-3.12985	2.67249	H	-1.12182	-1.4685	4.15646
C	-4.13225	-3.0553	4.0606	H	-2.85127	-2.38911	5.66535
C	-2.9838	-2.46364	4.58947	H	-5.1758	-3.59369	2.24963
C	-2.00043	-1.95261	3.73973	H	-3.43364	-2.68546	0.74332
H	-4.89819	-3.45248	4.72054	H	6.11295	0.8848	1.84438
N	1.19386	-0.99945	-1.76279	H	6.07944	-1.00036	-2.02552
C	2.29963	-1.18517	-2.66238	H	8.58488	0.77796	1.87267
C	2.65842	-0.15761	-3.54392	H	8.54785	-1.07614	-2.00914
C	3.69923	-0.34693	-4.45393	H	-6.15302	-0.83161	1.71485

C	4.39222	-1.56069	-4.49488	H	-6.03843	1.12317	-2.11591
C	4.03479	-2.5866	-3.61629	H	-8.60031	-0.74224	1.70124
C	2.99329	-2.40239	-2.70441	H	-8.49556	1.21912	-2.14115
H	5.20041	-1.70555	-5.2061	H	-12.20773	-0.35078	1.1313
C	-0.13882	1.85201	1.90018	H	-10.82011	-1.45928	1.23878
N	-1.23821	1.40264	1.30895	H	-10.77437	0.12832	2.06993
C	-2.41319	2.10097	1.76529	H	11.96647	-2.08334	0.19208
C	-3.289	1.51595	2.68761	H	10.47729	-2.32082	1.14458
C	-4.39138	2.23259	3.1549	H	10.46108	-2.56538	-0.62885
C	-4.63621	3.53337	2.70402	C	3.257	0.08336	-0.08006
C	-3.76125	4.11969	1.78757	C	4.4811	-0.00005	-0.09704
C	-2.6506	3.40911	1.32444	C	-3.2481	-0.0048	-0.14028
H	-5.49747	4.08589	3.06908	C	-4.47138	0.08326	-0.17497

Table S9. Cartesian coordinates of **1^{Cl}** ($E = -7801.19753803$ hartree).

C	8.71526	0.54266	0.36489	C	-6.61923	-0.8201	1.09589
C	8.06266	0.09178	-0.79116	C	-5.89381	-0.30443	0.00274
C	6.67303	-0.01382	-0.81942	C	-6.62939	0.10136	-1.1346
C	5.88524	0.32326	0.30047	C	-8.01355	-0.00556	-1.17226
C	6.55814	0.7745	1.45866	C	-8.72358	-0.52409	-0.07432
C	7.94249	0.88272	1.48983	C	-8.00851	-0.92991	1.06119
S	10.48332	0.71945	0.52149	S	-10.49774	-0.61419	-0.23574
C	11.12326	0.19626	-1.10426	C	-11.04802	-1.33549	1.34643
C	4.17685	1.63739	4.65797	H	0.21622	2.78367	-2.47725
C	3.52772	0.40404	4.59212	H	-0.27691	-2.82543	2.56593
C	2.52377	0.21315	3.64371	H	-3.51605	2.6015	-0.79447
C	2.16747	1.24404	2.76589	H	-5.24651	3.47606	-2.33383
C	2.83245	2.47434	2.84801	H	-2.75235	2.48725	-5.70062
C	3.83948	2.67681	3.79226	H	-1.03487	1.59615	-4.16129
N	1.09683	1.04616	1.82982	H	-3.069	-0.46425	-3.04141
C	0.06124	1.84082	2.04958	H	-4.97138	-1.77096	-3.95278
N	-1.10741	1.78954	1.39668	H	-3.66198	-5.21989	-1.73374
C	-1.98646	2.88748	1.61907	H	-1.75217	-3.90728	-0.84032
C	-1.50228	4.20671	1.58886	H	-2.1786	0.40491	3.55426
C	-2.35362	5.28624	1.82232	H	-4.04584	-0.10671	5.10649
C	-3.70102	5.0442	2.08271	H	-4.52086	-3.96307	3.25099
C	-4.20647	3.74356	2.10773	H	-2.66162	-3.43816	1.6958
C	-3.3497	2.66992	1.87378	H	-0.45839	4.39683	1.36082
Ru	-1.30445	0.24197	0.07405	H	-1.97199	6.30096	1.7913
Ru	1.29947	-0.22429	0.11116	H	-5.25749	3.56843	2.31101
N	1.04466	-1.89407	1.2651	H	-3.73626	1.65888	1.87747
C	1.91474	-3.01046	1.41938	H	3.64844	-1.81682	1.87389
C	1.4347	-4.31923	1.23944	H	5.15241	-3.76352	2.18866
C	2.2766	-5.41847	1.40516	H	1.8987	-6.42444	1.25865
C	3.61045	-5.20616	1.7483	H	0.40236	-4.48303	0.94728
C	4.11197	-3.91541	1.92214	H	0.14955	2.58426	2.84422
C	3.26466	-2.82194	1.755	H	2.57408	3.27357	2.16061
N	-1.13863	1.57397	-1.48204	H	4.35404	3.62987	3.84997

C	-2.14338	2.05752	-2.36267	H	3.79444	-0.39373	5.27689
C	-3.3485	2.57522	-1.86282	H	2.00567	-0.73718	3.59198
C	-4.32306	3.06623	-2.72865	H	1.77686	3.99822	-0.38142
C	-4.09763	3.03622	-4.10602	H	3.72211	5.38619	-1.05752
C	-2.91474	2.5186	-4.62871	H	5.14815	2.15595	-3.52061
C	-1.94445	2.0274	-3.75463	H	3.20968	0.77241	-2.82584
N	-1.15384	-1.36792	-1.37369	H	-0.09524	-2.49961	-2.74562
C	-0.02101	-1.7771	-1.93041	H	1.23449	-1.14885	-4.24339
N	1.20926	-1.39701	-1.57438	H	3.02278	-1.89151	-5.78147
C	2.25487	-1.79546	-2.45001	H	5.35016	-3.23077	-2.41638
C	3.43368	-2.36857	-1.94789	H	3.54956	-2.50391	-0.8809
C	4.44776	-2.77667	-2.81144	H	-6.09858	0.5053	-1.99105
C	4.28895	-2.60665	-4.18794	H	-6.0821	-1.13974	1.98353
C	3.13344	-2.03148	-4.71165	H	-8.55054	0.31508	-2.06156
C	2.12303	-1.6245	-3.83971	H	-8.52162	-1.33337	1.92708
N	-1.17909	-1.19203	1.66579	H	6.1836	-0.36633	-1.72218
C	-2.29301	-1.48179	2.52391	H	5.97915	1.04178	2.33713
C	-2.69519	-0.54512	3.48355	H	8.62526	-0.18029	-1.67735
C	-3.74329	-0.83068	4.35762	H	8.43041	1.2338	2.39575
C	-4.39025	-2.06353	4.26572	H	12.20938	0.29442	-1.03716
C	-4.00764	-3.00974	3.31603	H	10.87267	-0.84621	-1.31575
C	-2.95659	-2.71322	2.44778	H	10.75636	0.84313	-1.90501
C	0.10592	1.98464	-1.74145	H	-12.13611	-1.40397	1.27439
N	1.21294	1.52003	-1.17619	H	-10.63731	-2.33759	1.49292
C	2.36895	2.28873	-1.55027	H	-10.78733	-0.69282	2.19097
C	3.32452	1.77661	-2.43615	C	-3.25202	-0.05708	0.04432
C	4.41366	2.55282	-2.82817	C	-4.47147	-0.19261	0.03733
C	4.54897	3.84605	-2.32174	C	3.24517	0.0741	0.20137
C	3.61086	4.37736	-1.4401	C	4.46313	0.20991	0.26184
C	2.5189	3.59289	-1.06239	Cl	5.92874	4.82815	-2.81471
C	-2.28957	-2.09493	-1.8726	Cl	-5.33082	3.65831	-5.20002
C	-3.20198	-1.49969	-2.75197	Cl	4.68218	-6.58766	1.9567
C	-4.27054	-2.23251	-3.26556	Cl	-5.71306	-2.43128	5.37131
C	-4.42887	-3.56648	-2.88781	Cl	5.57252	-3.12353	-5.27895
C	-3.5335	-4.18033	-2.01534	Cl	5.44357	1.88582	5.85813
C	-2.46156	-3.43802	-1.51506	Cl	-5.78269	-4.49394	-3.53437
C	-0.15317	-2.00707	1.85402	Cl	-4.78457	6.40091	2.37564

Table S10. Cartesian coordinates of **1^{CF3}** ($E = -6820.73974559$ hartree).

Ru	-0.56424	-1.40356	6.15583	C	-5.21242	-4.30191	6.49193
N	-0.89179	-3.05934	7.32936	C	-6.40882	-4.80823	6.99086
N	-0.27828	-2.74157	4.46279	C	-6.86714	-4.41742	8.25414
N	-0.50063	0.27374	4.82109	C	-6.1145	-3.52757	9.02333
N	-1.16255	-0.20993	7.70313	C	-4.9107	-3.02872	8.52673
C	-2.17021	-3.43006	7.44475	H	-4.32124	-2.33902	9.12274
C	-1.34778	0.45907	3.82054	H	-6.46295	-3.22219	10.00424
C	2.62612	-1.2952	6.3342	H	-6.98972	-5.50324	6.39355
C	1.4023	-1.33021	6.2615	H	-4.85875	-4.60277	5.51357
C	0.05574	-3.90513	7.96442	H	-0.96924	-4.08234	3.0457
C	1.08406	-3.36512	8.75359	C	-3.43465	-3.96811	3.2432
C	2.00363	-4.2022	9.37558	C	-4.51647	-3.48245	2.49052
C	1.91779	-5.59082	9.21744	C	-5.36456	-4.36575	1.83164
C	0.9005	-6.13769	8.43322	C	-5.15326	-5.74738	1.91584
C	-0.02325	-5.30096	7.80948	C	-4.08428	-6.24037	2.66648
C	1.02393	-3.12782	3.98776	C	-3.23439	-5.3579	3.33052
C	1.78991	-4.07326	4.68059	H	-2.42826	-5.74949	3.94291
C	3.0416	-4.44697	4.20115	H	-3.92227	-7.30951	2.75018
C	3.54407	-3.87639	3.02632	H	-6.19504	-3.97776	1.25074
C	2.77548	-2.94929	2.3192	H	-4.68321	-2.4162	2.42243
C	1.51609	-2.58451	2.79503	C	-6.04935	-6.68376	1.15809
C	0.60343	1.18819	4.81145	C	-8.13386	-5.00682	8.80454
C	0.78767	2.06857	5.88457	C	-7.83889	3.48821	6.607
C	1.85293	2.96529	5.88122	C	-5.05251	0.49877	-1.42933
C	2.74105	2.99325	4.80125	C	3.94806	3.8847	4.83513
C	2.55109	2.12937	3.71862	C	1.30375	0.67012	12.79932
C	1.4859	1.2331	3.72309	C	4.93345	-4.21682	2.5697
C	-0.54464	-0.01363	8.96956	C	2.96085	-6.4743	9.83792
C	-1.28927	-0.14958	10.1547	F	-5.55068	-0.68422	-1.86818
C	-0.68914	0.05767	11.39425	F	-4.20765	0.94187	-2.38763
C	0.66456	0.39435	11.46807	F	-6.09379	1.36022	-1.37859
C	1.41461	0.51895	10.29354	F	-7.64122	4.68835	6.01809
C	0.81839	0.3136	9.05306	F	-8.83769	2.87855	5.91099
H	-2.38855	-4.22679	8.15818	F	-8.32241	3.71949	7.84722
H	-1.10698	1.22771	3.08388	F	-8.72797	-4.19087	9.70473
H	1.14994	-2.29396	8.88538	F	-9.03962	-5.26213	7.83239
H	2.78429	-3.77375	9.99581	F	-7.9096	-6.18522	9.43968
H	0.8287	-7.21194	8.30195	F	-6.04382	-7.93167	1.67824
H	-0.79466	-5.73073	7.17813	F	-5.67545	-6.80182	-0.1408
H	1.40214	-4.51123	5.5925	F	-7.33386	-6.25654	1.14855
H	3.62744	-5.18336	4.74122	F	5.2589	-5.50127	2.84225
H	3.15108	-2.51816	1.39735	F	5.09739	-4.03232	1.24048
H	0.91228	-1.87219	2.24213	F	5.8683	-3.44545	3.18567
H	0.09281	2.05061	6.71549	F	4.28935	4.32862	3.60453
H	1.98822	3.64625	6.71467	F	3.76617	4.96821	5.62083
H	3.23428	2.15162	2.876	F	5.03744	3.23049	5.32257
H	1.35123	0.54903	2.89207	F	1.24189	1.98553	13.12473
H	-2.33291	-0.44326	10.10922	F	2.61296	0.33127	12.81273

H	-1.27282	-0.06049	12.30086	F	0.70091	-0.00556	13.80345
H	2.46836	0.77222	10.34604	F	3.35703	-6.01676	11.04825
H	1.40387	0.39188	8.14626	F	4.07857	-6.54752	9.07114
Ru	-3.0092	-1.49691	5.15045	F	2.52401	-7.74205	10.00897
N	-2.55879	-3.0743	3.9129	C	4.05083	-1.33548	6.40083
C	-1.25283	-3.33143	3.78558	C	4.71632	-2.51143	6.81164
N	-3.19392	-2.90655	6.78262	C	4.83787	-0.22493	6.02381
N	-3.19436	0.13126	6.54259	C	6.10619	-2.58914	6.79568
C	-2.36583	0.35959	7.54815	H	4.13032	-3.37044	7.12254
N	-2.5008	-0.20032	3.65212	C	6.2273	-0.30254	6.0202
C	-4.97517	-1.52337	5.0322	H	4.35365	0.69985	5.73002
C	-6.1948	-1.5293	4.8999	C	6.87597	-1.49264	6.38233
C	-3.13599	-0.01792	2.39075	H	6.59961	-3.51027	7.09136
C	-2.3922	-0.11572	1.20234	H	6.8114	0.56439	5.72448
C	-3.00687	0.07251	-0.03329	C	-7.60703	-1.55463	4.69526
C	-4.3726	0.35812	-0.09718	C	-8.2585	-2.72138	4.24525
C	-5.12	0.4518	1.08214	C	-8.40453	-0.41192	4.93046
C	-4.50941	0.26346	2.31837	C	-9.6372	-2.75242	4.04191
H	-5.08913	0.32597	3.2298	H	-7.67125	-3.61353	4.05057
H	-6.17944	0.68163	1.03698	C	-9.77811	-0.43954	4.73057
H	-2.42187	-0.00631	-0.94334	H	-7.93751	0.50472	5.27199
H	-1.33555	-0.35918	1.24388	C	-10.41538	-1.61109	4.28378
H	-2.66708	1.0898	8.30145	H	-10.09306	-3.67299	3.69468
C	-4.35718	0.97258	6.56818	H	-10.36029	0.45804	4.92385
C	-4.54441	1.93055	5.56435	S	8.66525	-1.62423	6.32493
C	-5.65781	2.7661	5.59307	S	-12.18258	-1.5291	4.06192
C	-6.59162	2.65311	6.62864	C	-12.63265	-3.19977	3.48516
C	-6.40151	1.70765	7.64042	H	-13.71543	-3.17792	3.34062
C	-5.28698	0.87281	7.61133	H	-12.15135	-3.43685	2.53312
H	-5.1465	0.12735	8.38705	H	-12.38866	-3.95939	4.23191
H	-7.12102	1.62012	8.44757	C	8.93078	-1.78012	4.5122
H	-5.79437	3.51085	4.81608	H	9.99706	-1.97213	4.36528
H	-3.81375	2.02277	4.7695	H	8.3497	-2.61464	4.11248
C	-4.45437	-3.40695	7.25725	H	8.65681	-0.85611	3.99731

IV. References

- [1] A. B. Pangborn, M. A. Giardello, R. H. Grubbs, R. K. Rosen, F. J. Timmers, *Organometallics* **1996**, *15*, 1518–1520.
- [2] L.-Y. Zhang, P. Duan, J.-Y. Wang, Q.-C. Zhang, Z.-N. Chen, *J. Phys. Chem. C* **2019**, *123*, 5282–5288.
- [3] C. Lin, J. D. Protasiewicz, E. T. Smith, T. Ren, *Inorg. Chem.* **1996**, *35*, 6422–6428.
- [4] T. A. Stephenson, G. Wilkinson, *J. Inorg. Nucl. Chem.* **1966**, *28*, 2285–2291.
- [5] C. Lin, T. Ren, E. J. Valente, J. D. Zubkowski, E. T. Smith, *Chem. Lett.* **1997**, *26*, 753–754.
- [6] Rigaku Oxford Diffraction, CrysAlisPro, Rigaku Corporation, Tokyo, Japan. 2015.
- [7] O. V. Dolomanov, L. J. Bourhis, R. J. Gildea, J. a. K. Howard, H. Puschmann, *J Appl Cryst* **2009**, *42*, 339–341.
- [8] G. M. Sheldrick, *Acta Cryst A* **2015**, *71*, 3–8.
- [9] G. M. Sheldrick, *Acta Cryst C* **2015**, *71*, 3–8.
- [10] Gaussian 16, Revision C.01, M. J. Frisch, G. W. Trucks, H. B. Schlegel, G. E. Scuseria, M. A. Robb, J. R. Cheeseman, G. Scalmani, V. Barone, G. A. Petersson, H. Nakatsuji, X. Li, M. Caricato, A. V. Marenich, J. Bloino, B. G. Janesko, R. Gomperts, B. Mennucci, H. P. Hratchian, J. V. Ortiz, A. F. Izmaylov, J. L. Sonnenberg, D. Williams-Young, F. Ding, F. Lipparini, F. Egidi, J. Goings, B. Peng, A. Petrone, T. Henderson, D. Ranasinghe, V. G. Zakrzewski, J. Gao, N. Rega, G. Zheng, W. Liang, M. Hada, M. Ehara, K. Toyota, R. Fukuda, J. Hasegawa, M. Ishida, T. Nakajima, Y. Honda, O. Kitao, H. Nakai, T. Vreven, K. Throssell, J. A. Montgomery, Jr., J. E. Peralta, F. Ogliaro, M. J. Bearpark, J. J. Heyd, E. N. Brothers, K. N. Kudin, V. N. Staroverov, T. A. Keith, R. Kobayashi, J. Normand, K. Raghavachari, A. P. Rendell, J. C. Burant, S. S. Iyengar, J. Tomasi, M. Cossi, J. M. Millam, M. Klene, C. Adamo, R. Cammi, J. W. Ochterski, R. L. Martin, K. Morokuma, O. Farkas, J. B. Foresman, and D. J. Fox, Gaussian, Inc., Wallingford CT, 2016., **n.d.**
- [11] R. L. Martin, *J. Chem. Phys.* **2003**, *118*, 4775–4777.
- [12] C. Lin, T. Ren, E. J. Valente, J. D. Zubkowski, *J. Chem. Soc., Dalton Trans.* **1998**, 571–576.
- [13] I. P.-C. Liu, T. Ren, *Inorg. Chem.* **2009**, *48*, 5608–5610.
- [14] M. Brandbyge, J.-L. Mozos, P. Ordejón, J. Taylor, K. Stokbro, *Phys. Rev. B* **2002**, *65*, 165401.
- [15] J. P. Perdew, K. Burke, M. Ernzerhof, *Phys. Rev. Lett.* **1996**, *77*, 3865–3868.

- [16] M. Paulsson, M. Brandbyge, *Phys. Rev. B* **2007**, *76*, 115117.
- [17] T. Tada, M. Kondo, K. Yoshizawa, *J. Chem. Phys.* **2004**, *121*, 8050–8057.
- [18] Gaussian 09, Revision D.01, M. J. Frisch, G. W. Trucks, H. B. Schlegel, G. E. Scuseria, M. A. Robb, J. R. Cheeseman, G. Scalmani, V. Barone, G. A. Petersson, H. Nakatsuji, X. Li, M. Caricato, A. Marenich, J. Bloino, B. G. Janesko, R. Gomperts, B. Mennucci, H. P. Hratchian, J. V. Ortiz, A. F. Izmaylov, J. L. Sonnenberg, D. Williams-Young, F. Ding, F. Lipparini, F. Egidi, J. Goings, B. Peng, A. Petrone, T. Henderson, D. Ranasinghe, V. G. Zakrzewski, J. Gao, N. Rega, G. Zheng, W. Liang, M. Hada, M. Ehara, K. Toyota, R. Fukuda, J. Hasegawa, M. Ishida, T. Nakajima, Y. Honda, O. Kitao, H. Nakai, T. Vreven, K. Throssell, J. A. Montgomery, Jr., J. E. Peralta, F. Ogliaro, M. Bearpark, J. J. Heyd, E. Brothers, K. N. Kudin, V. N. Staroverov, T. Keith, R. Kobayashi, J. Normand, K. Raghavachari, A. Rendell, J. C. Burant, S. S. Iyengar, J. Tomasi, M. Cossi, J. M. Millam, M. Klene, C. Adamo, R. Cammi, J. W. Ochterski, R. L. Martin, K. Morokuma, O. Farkas, J. B. Foresman, and D. J. Fox, Gaussian, Inc., Wallingford CT, can be found under <https://gaussian.com/g09citation/>, **2016**.
- [19] K. Sugimoto, Y. Tanaka, S. Fujii, T. Tada, M. Kiguchi, M. Akita, *Chem. Commun.* **2016**, *52*, 5796–5799.